UNIVERSITÀ
DEGLI STUDI
DI PADOVA

UNIVERSITA' DEGLI STUDI DI PADOVA

Dipartimento di Ingegneria Industriale DII

Corso di Laurea Magistrale in Ingegneria Meccanica

Optimal routing and design of CO_2 based district anergy networks

Relatore
Andrea Lazzaretto
UNIVERSITA' DEGLI STUDI DI PADOVA

Co-Relatore
Luc Girardin, François Maréchal
EPFL

Studente
Andrea Valle

Matricola
1211613

Anno Accademico 2021/2022

Abstract

One of the main global goals in the context of the rapid climate change is the reduction of the energy consumption. Among the most interesting sectors, with an important margin of improvement, it is possible to find the urban areas. Urban areas are mainly composed of residential buildings, where is well established the district energy network as the best way for heat distribution. The district network is a grid of pipes driving a working fluid and connecting the buildings among each other, in order to share thermal energy.
The evolution of this system relies on two aspects, reducing the temperature of the working fluid and lately moving from water to refrigerants, in order to reach a more efficient system. In the past two decades the CO_2 has faced a growing popularity as a refrigerant, joining the hydrocarbon and HFO as the present and next generation of working fluids. The present work investigates the CO_2 network, which exploits the latent heat of the carbon dioxide near the saturation state in a vapour and liquid pipes to transfer heat to the users. The CO_2 has been chosen for the fact that it is the only non-flammable, non-toxic, natural refrigerant available with the most appropriate range of temperatures. This work presents a method meant for decision makers to implement a district energy network based on CO_2 in a neighborhood, in this way the best design alternatives are evaluated before making a decision. The method is characterized by two branches, in order to achieve the network topology design first and secondly to cross the results with the optimization of the energetic model. The network design relies on a MILP problem, in order to develop a tree graph, which connects the buildings to the available pathway of the neighborhood. The problem consists of a system of equations which is fed by the most severe energy demand of each building, the starting point of the graph and the streets of the district are taken as the available path to place the network. Moreover a bunch of options are approached in order to develop a set of configurations, among which there are the variation of the starting point of the graph and the adoption of a discrete variable as the power assigned to the centralized feeding technology of the network.
The results of the network design are merged with the optimization of a set of conversion technologies, where it is simulated the whole neighborhood by splitting the buildings connected to the network with the heat pumps to the ones disconnected and with standalone technology. The set of conversion technologies includes the PV panels, the network based heat pumps, the central plant, the electrical heater, the ground source heat pump (GSHP), the decentralize refrigeration, the power-to-gas and the storages composed by batteries and CO_2 tanks. Furthermore, to fully exploit the potential of the district network based on a refrigerant is integrated in order to achieve the waste heat recovery of a data center.
The validation of the method is carried out by the case study about the district of Ronquoz in Sion (Switzerland), which is going to face a complete requalification in the following years. The implementation of the method results in a minimum of the cost for a district network that covers 80% of the neighborhood. The connection of the data center voids the investment cost of the dedicated refrigeration system, while the total operating cost increases by the 95%.

Contents

Listing of figures

Listing of tables

Listing of acronyms

T_{ext}	Outdoor temperature
SH	Space heating
DHW	Domestic hot water
c_p	Specific heat capacity
ΔT_{ln}	Logarithmic mean temperature difference
$MILP$	Mixed Integer Linear Programming
DN	District Network
ERA	Energy Reference Area
GIS	Geographic Information System
COP	Coefficient Of Performance
$AMPL$	A Mathematical Programming Language
$SOFC - GT$	Solid Oxide Fuel Cell - Gas Turbine
$SOEC$	Solid Oxide Electrolyzer Cell
PV	Photovoltaic
CPW	Capex weight factor
PUE	Power Usage Effectiveness
ERE	Energy Reuse Effectiveness
ERF	Energy Reuse Factor
$GSHP$	Ground Source Heat Pump
OC	Operating cost
IC	Investment cost
ρ	Density
$\dot{m}$	Mass flow rate
ΔP	Pressure loss

1 Introduction

The energy consumption is globally growing and in particular the increased quality of human life is affecting more and more the growth. This trend is going hand in hand with the urban development, since about the 56% of the global population lives in urban areas with an average growth of the 0.45% per year in the last two decades, with no evidence of decline [2].
In this context the urban areas have been targeted as the main challenge in terms of energy consumption, covering at the moment the 40% of the total amount in Europe, so it is emerging an important potential chance of energy savings [3]. The approach for achieving this opportunity could be developed in different ways, but for reaching the best results a mix of improving the energy efficiency of the buildings and a better integration of electrical and thermal energies have the greatest benefits from the thermoeconomic point of view.
This work proposes a method for the integration of the district energy network into a neighborhood. The network is a grid of pipes driving a working fluid and connecting the buildings among each other, in order to share thermal energy. This system relies on centralized plants for feeding the whole system and decentralized technologies for proving the on-site energy requirements of each building. One of the most interesting upside of the district network is the opportunity to take advantage of every available energy source in that specific area (e.g. harvesting/dissipate heat from/to the environment or the ground, converting solar energy and gathering the excess of heat).
The main decentralized technologies are the heat pumps (HPs), since they can count on harvesting heat from the DN and delivering it by assuring the most appropriate temperatures with a reasonable high efficiency, or the other way around by using the buildings as a heat source and the DN as a heat sink for ensuring the right amount of cooling. The parameter that quantify the performance of a heat pump is the COP (coefficient of performance), which is the ratio between useful heating or cooling provided

and work that is required. In the case the network is used as heat source, despite it is relative cold, the temperature of the network is still high for the heat pumps to have a higher COP than adopting natural source. This is critical advantage, since the buildings need different temperature o heat distribution, so each HP can work at its best COP. For the network as heat sink, is the other way around.
HPs could be even installed for self-sufficient buildings [4], but harvesting heat from the environment requires a trans-critical cycle for an optimal performance, considering the refrigerants treated in this work. So, the storage technologies aren't particularly attractive, since they cannot exploit their full potential [4]. Moreover, this technology faces an improvement of the consumption of electricity for delivering the same service, which means a lower COP compared to coefficient for the HPs connected to the network. A lower COP is due to a not optimal exploiting of other natural sources as heat sink or source, e.g. environment and ground.
Achieving an higher efficiency for providing energy is, generally speaking, driving to a reduction of the greenhouse gas emissions, that Switzerland is pursuing to reduce of the 50% by the 2030 compared to the emissions of 2008 and reaching a zero-net by 2050 [5].
In this context the district network could play a key role by matching a superstructure of the available technologies and taking advantage of renewable energies. An even more integrated system should couple the sources with different type of storages to smooth the fluctuations on which the natural resources are dependent. All these aspects would bring the whole system to a higher self-sufficiency, reducing the economic risk of buying electricity and natural gas from the market.
The district heating and cooling networks have been used for a long time, going through a development that is interesting to explain for fixing the new goals about the future developments. The DN haven't been implemented until the 1930s, since previously for heating up buildings and providing heat to industrial processes were used steam coming from large high pressure boilers or group of boilers, straight located on-site at the demand [6]. Just after this period it has been developed the first generation of district heating and cooling networks, which were injecting steam and chilled water through the pipes, allowing heat exchanges for space heating, space cooling and industrial processes. These first networks were fed by a large plant operating near the maximum capacities, which is an efficient solution just when the energy demand is constant along the time [6].
The second generation used pressurized water, that was matched with co-generation plants for heat and power production, while keeping the temperature of the operating fluid below 100 °C. In parallel there were installed the pipes for delivering cold water, which were fed by large scale mechanical chillers [7] to satisfy the cooling demand.
Similarly, also the third generation of heating systems used pressurized water, but focusing on the reduction of the supply temperature, for leading the system to an efficiency improvement. In the 90s, the cooling pipes were still fed by cold water, with the difference of the adoption of a wider set of technologies as central plant, exploiting the potential of using lakes as a source for direct cooling [7].

The aim of the fourth generation was to decrease the grid losses by drastically reducing the operating temperature of the networks. In this scenario begins to have an high importance also the ability to recover waste heat and also introducing the concept of smart energy systems, which integrates renewable sources [7]. A low-temperature grid prefers a match with a comparable temperature demand, so a further improvement is also required from the utilities by decreasing both space heating (SH) and domestic hot water (DHW). The DHW is usually stored with on-site tanks for providing it instantaneously to the users and due to a lower temperature is the perfect condition for the development legionella bacteria, so this storages must be reduced for avoiding this issue.
The integration of an increasing number of technologies implies the coordination of the energy fluctuation, especially about renewable sources (e.g. photovoltaic, wind, wave), so storages of different types (e.g. thermal, electrical, chemical) are necessary for balancing the system or other constant energy suppliers [7].
The latest development is the fifth generation (5G), which has the possibility to combine heating and cooling requirements with a refrigerant based network. This technology relies on latent heat of evaporation/condensation [8], in order to store and transfer thermal energy, instead of the sensible heat as previously done. The economical feasibility of the 5G is proved in [8], were the CO_2 and $R1234yf$ are targeted as the most attractive working fluids for their electricity requirements. In support to this, their pipes compactness can bring a relevant economical advantage compared to a water DN, as soon as the safety and regulatory issues due to the high working pressure will be solved [8]. The focus of this work is on the CO_2, since it is non-toxic, non-flammable and available in the nature. In the past two decades the CO_2 has faced a growing popularity as a refrigerants since the article of Lorentzen [9], joing the hydrocarbon and HFO as the next and present generation of refrigerants.
The profitability perspective has been proven in the work of Henchoz and al. [10], where a CO_2 plant is potentially bringing a reduction of the energy consumption of 84.4% compared to the present system based on gas boilers and chiller.

1.1 Contributions and novelty

After having mastered all the previous information, it must be claimed the research question of the present work:

- How to identify the optimal pathway and designing the future networks, by integrating and sizing a superstructure of technologies?

In order to accomplish this task is proposed a method to estimate both the network design and the optimization of the energetic model. The main novelty of the method is about a different prospective,

since differently from the other works in the literature, it hasn't been optimized a neighborhood keeping all the buildings connected to the DN, but a progressive set of networks' layout are generated based on a growing power coming from the centralized feeding system. Furthermore, a deep set of energy conversion technologies is integrated, in order to smooth the energy fluctuations which are one of the main issue of the renewable energies.

The following question summerized the sections that this master thesis is going to carry out, for giving a general overview to the reader.

- **Chapter 2: Definition of the method**
  This chapter describes a method for designing the integration of an energetic system with 5G district network, starting from a set of rough geospatial information (e.g. natural resource available and buildings' data) and the available pathway for the pipes installation.

- **Chapter 3: Estimating the energy demand**
  In this section it has been adopted the energy signature model for retrieving the building energy demand. The model takes into consideration a broad mix of building typology to gather different types of the energy requirements: space heating (SH), air cooling (AC), domestic hot water (DHW), refrigeration (REF) and electricity (EL).
  The energy signature, a linear regressive technique, is implemented to the neighborhood of Ronquoz in the city of Sion (Switzerland), which is going to face a complete requalification in the following years.
  Here is also provided the estimation of the energy demand in extreme conditions.

- **Chapter 4: Network design**
  In the fourth chapter is defined a MILP problem for the construction of the network as a tree graph, adopting CO_2 as a working fluid and relying on the available streets of the neighborhood. The linear objective function is the investment cost of the pipes, which is function of the sections and the lengths of the segments. Moreover, in the post-process the results are then refined with the non-linear cost function, estimating also the operating cost of keeping the whole network at the working pressure.
  This process is interesting for developing different considerations with the goal of reaching the problem's optimal, e.g. expanding the network through the district, moving the starting point of the graph and matching a pre-installed DN of the same typology.

- **Chapter 5: Energetic model**
  The fifth chapter sets up the superstructure of available technologies for modelling the whole neighborhood integrating the 5G district network, assessing the options for renewable sources in the specific area, e.g. the geothermal, solar and harvesting heat from the cooling system of a data center. Moreover, this section takes care of the waste heat recovery of a data center.

Introduzione

Il consumo di energia sta crescendo globalmente e in particolare l'aumento della qualità della vita umana sta influenzando sempre più la crescita. Questa tendenza va di pari passo con lo sviluppo urbano, dato che circa il 56% della popolazione globale vive in aree urbane con una crescita media dello 0,45% all'anno negli ultimi due decenni, senza prove di declino [2]. In questo contesto le aree urbane sono state scelte come la principale sfida in termini di consumo di energia, coprendo al momento il 40% della quantità totale in Europa, quindi si prospetta un'importante possibilità potenziale di risparmio energetico [3]. L'approccio per raggiungere questa opportunità può essere sviluppato in diversi modi, ma per ottenere i migliori risultati un mix di miglioramento dell'efficienza energetica degli edifici e una migliore integrazione delle energie elettriche e termiche hanno i maggiori benefici dal punto di vista termoeconomico. Questo lavoro propone un metodo per l'integrazione della rete di teleriscaldamento in un quartiere. La rete è una griglia di tubi dove fluisce un fluido operativo e che collega gli edifici tra loro, al fine di condividere l'energia termica. Questo sistema si basa su un impianto centralizzato che alimenta l'intero sistema e su tecnologie decentralizzate per fornire il fabbisogno energetico in loco di ogni edificio. Uno degli aspetti più interessanti di un impianto di teleriscaldamento è l'opportunità di sfruttare ogni fonte di energia disponibile in quell'area specifica (ad esempio raccogliere/diffondere il calore dall'ambiente o dal terreno, convertire l'energia solare e raccogliere l'eccesso di calore).

Le principali tecnologie decentralizzate sono le pompe di calore (HP), dato che possono contare sulla dalla rete di teleriscaldamento come sorgente termica, assicurando le temperature più appropriate con un'efficienza ragionevolmente alta, o il contrario, utilizzando gli edifici come fonte di calore e la rete come dissipatore di calore per assicurare la giusta quantità di raffreddamento. Il parametro che quantifica le prestazioni di una pompa di calore è il COP (coefficient of performance), che è il rapporto tra il riscaldamento o il raffreddamento utile fornito e il lavoro richiesto. Nel caso in cui la rete venga utilizzata come sorgente di calore, nonostante sia relativamente freddo, la temperatura della rete è ancora alta per le pompe di calore in modo da avere un COP più alto rispetto all'adozione di fonti naturali. Questo è un vantaggio molto importante, dal momento che gli edifici hanno bisogno di temperature diverse di distribuzione del calore, quindi ogni HP può lavorare al suo COP ottimale. Per la rete come dissipatore di calore, è il contrario.

Gli HP potrebbero anche essere installati per edifici autosufficienti [4], ma la raccolta di calore dall'ambiente richiede un ciclo transcritico per una prestazione ottimale, considerando i refrigeranti trattati in questo lavoro. Quindi, le tecnologie di stoccaggio non sono particolarmente attraenti, poiché non possono essere sfruttate al meglio [4]. Inoltre questa tecnologia conduce a un aumento del consumo di elettricità

per fornire lo stesso servizio, il che significa un COP inferiore rispetto al coefficiente per gli HP collegati alla rete. Un COP più basso è dovuto a uno sfruttamento non ottimale di altre fonti naturali come dissipatore o sorgente di calore, per esempio l'aria esterna e il terreno.
Raggiungere una maggiore efficienza per la fornitura di energia vuol dire, in generale, portare a una riduzione delle emissioni di gas a effetto serra, in cui la Svizzera sta perseguendo per arrivare a ridurre del 50% entro il 2030 rispetto alle emissioni del 2008 e raggiungere un zero-net entro il 2050 [5].
In questo contesto la rete di teleriscaldamento potrebbe giocare un ruolo chiave, abbinando una superstruttura delle tecnologie di conversione energetica disponibili e sfruttando le energie rinnovabili. Un sistema ancora più integrato dovrebbe accoppiare le fonti con diversi tipi di immagazzinamento per attenuare le fluttuazioni da cui dipendono le risorse naturali. Tutti questi aspetti porterebbero l'intero sistema a una maggiore autosufficienza, riducendo il rischio economico di comprare elettricità e gas naturale dal mercato.
Le reti di teleriscaldamento sono state utilizzate per molto tempo, passando attraverso uno sviluppo che è interessante analizzare per fissare i nuovi obiettivi riguardo agli sviluppi futuri.
Le reti di teleriscaldamento non sono state implementate fino al 1930, poiché, in precedenza, per il riscaldamento degli edifici e la fornitura di calore ai processi industriali si utilizzava il vapore proveniente da grandi caldaie ad alta pressione o di gruppi di caldaie, direttamente situate in loco presso la domanda [6].
Subito dopo questo periodo è stata sviluppata la prima generazione di reti di teleriscaldamento e raffreddamento, che iniettavano vapore e acqua refrigerata attraverso i tubi, permettendo scambi di calore per il riscaldamento e il raffreddamento degli edifici e per i processi industriali. Queste prime reti erano alimentate da un grande impianto che operava vicino alle capacità massime, che è una soluzione efficiente solo quando la domanda di energia è costante nel tempo [6].
La seconda generazione utilizzava acqua pressurizzata, che veniva abbinata a impianti di cogenerazione per la produzione di calore ed energia elettrica, mantenendo la temperatura del fluido operativo sotto i 100 °C. In parallelo sono state installate le tubazioni per la fornitura di acqua fredda, che venivano alimentate da refrigeratori meccanici su larga scala [7] per soddisfare la domanda di raffreddamento.
Allo stesso modo, anche la terza generazione di sistemi di riscaldamento utilizzava acqua pressurizzata, ma puntando sulla riduzione della temperatura di alimentazione, per portare il sistema ad un miglioramento dell'efficienza. Negli anni '90, i tubi di raffreddamento erano ancora alimentati da acqua fredda, con la differenza dell'adozione di un insieme più ampio di tecnologie come impianto di alimentazione centralizzato, sfruttando il potenziale dell'uso dei laghi come fonte di raffreddamento diretto [7].
L'obiettivo della quarta generazione era quello di diminuire le perdite di rete riducendo drasticamente la temperatura del fluido operativo delle reti. In questo scenario inizia ad avere una grande importanza anche la capacità di recuperare il calore residuo e anche l'introduzione del concetto di sistemi energetici intelligenti, che integra le fonti rinnovabili [7]. Una rete a bassa temperatura preferisce una corrispondenza con una domanda di temperatura comparabile, quindi un ulteriore miglioramento è richiesto

anche dalle utenze, diminuendo sia il riscaldamento degli spazi (SH) che l'acqua calda sanitaria (DHW). L'acqua calda sanitaria è di solito immagazzinata con serbatoi in loco per fornirla istantaneamente agli utenti e a causa di una temperatura più bassa è la condizione perfetta per lo sviluppo dei batteri della legionella, quindi questo stoccaggio deve essere ridotto per evitare questo problema.
L'integrazione di un numero crescente di tecnologie implica il bilanciamento della fluttuazione dell'energia, soprattutto per quanto riguarda le fonti rinnovabili (ad esempio fotovoltaico, eolico, moto ondoso), quindi sono necessari stoccaggi di diversi tipi (ad esempio termico, elettrico, chimico) per bilanciare il sistema o altri fornitori di energia costante [7]. L'ultimo sviluppo è la quinta generazione (5G), che ha la possibilità di combinare i requisiti di riscaldamento e raffreddamento con una rete basata su un fluido refrigerante. Questa tecnologia si basa sul calore latente di evaporazione/condensazione [8], al fine di immagazzinare e trasferire energia termica, invece del calore sensibile come fatto in precedenza. La fattibilità economica della 5G è dimostrata in [8], dove CO_2 e $R1234yf$ sono analizzati come i fluidi refrigeranti più attraenti per le loro esigenze di elettricità. A sostegno di questo, la compattezza dei loro tubi può portare un vantaggio economico rilevante rispetto alle reti utilizzanti acqua, non appena le questioni di sicurezza e di regolamentazione dovute all'alta pressione di lavoro saranno risolte [8]. Il focus di questo lavoro è la CO_2, poiché non è tossica, non è infiammabile e disponibile in natura. Negli ultimi due decenni la CO_2 ha visto una crescente popolarità come refrigerante dopo l'articolo di Lorentzen [9], aggungendola a l'idrocarburi e l'HFO come la prossima e attuale generazione di refrigeranti.
La prospettiva di redditività è stata dimostrata nel lavoro di Henchoz [10], dove un impianto a CO_2 porta potenzialmente a una riduzione del consumo di energia dell'84,4

1.2 Contributi e novelt\u00e0

Dopo aver padroneggiato tutte le informazioni precedenti, si deve affermare la domanda di ricerca del presente lavoro:

- Come identificare il percorso ottimale e progettare le reti del futuro, integrando e dimensionando una superstruttura di tecnologie?

Per realizzare questo compito viene proposto un metodo per valutare sia la progettazione della rete che l'ottimizzazione del modello energetico. La principale novità del metodo riguarda una prospettiva diversa, poiché diversamente dagli altri lavori in letteratura, non è stato ottimizzato un quartiere mantenendo tutti gli edifici collegati alla rete, ma viene generato un insieme progressivo di layout di reti basato su una potenza crescente proveniente dal sistema di alimentazione centralizzato. Inoltre, viene integrato un ampio insieme di tecnologie di conversione dell'energia, al fine di attenuare le fluttuazioni di energia che sono uno dei problemi principali delle energie rinnovabili.

La seguente domanda riassume le sezioni che questa tesi magistrale realizzerà, per dare una visione generale al lettore.

- **Capitolo 2: Definizione del metodo**
  Questo capitolo descrive un metodo per progettare l'integrazione di un sistema energetico con la rete di telericaldamento 5G, partendo da un insieme di informazioni geospaziali grezze (ad esempio, dati sulle risorse naturali disponibili e sugli edifici) e il percorso disponibile per l'installazione dei tubi.

- **Capitolo 3: Stima della domanda energetica**
  In questa sezione è stato adottato il "energy signature model" per ottenere la domanda di energia degli edifici. Il modello prende in considerazione un ampio mix di tipologie di edifici per raccogliere diversi tipi di requisiti energetici: riscaldamento degli spazi (SH), raffreddamento dell'aria (AC), acqua calda sanitaria (DHW), refrigerazione (REF) ed elettricità (EL).
  Il "energy signature model", una tecnica lineare regressiva, è implementata al quartiere di Ronquoz nella città di Sion (Svizzera), che sta per affrontare una riqualificazione completa nei prossimi anni.

- **Capitolo 4: Progettazione della rete**
  Nel quarto capitolo viene definito un problema MILP per la costruzione della rete come un grafo, adottando CO_2 come fluido operativo e contando sulle strade disponibili del quartiere. La funzione obiettivo lineare è il costo di investimento dei tubi, che è funzione delle sezioni e delle lunghezze dei segmenti. Inoltre, nel post-processo i risultati sono poi raffinati con la funzione di costo non lineare, stimando anche il costo operativo per mantenere l'intera rete alla pressione operativa.
  Questo processo è interessante per sviluppare diverse considerazioni con l'obiettivo di raggiungere la configurazione ottimale del problema, ad esempio espandendo la rete attraverso il distretto, spostando il punto di partenza del grafo e considerando una parte di rete precedentemente installata.

- **Capitolo 5: Modello energetico**
  Il quinto capitolo configura la superstruttura delle tecnologie di conversione disponibili per modellare l'intero quartiere che integra la rete di teleriscalndamento 5G, valutando le opzioni per le fonti rinnovabili nell'area interessata, ad esempio il geotermico, il fotovoltaico e la raccolta di calore da un impianto di raffreddamento di un data center. Inoltre, questa sezione si occupa del recupero del calore residuo di un data center.

2

Method

The integration of the district network's design and the energetic model based on a predefined superstructure of technologies requires a method for reaching a reliable analysis at the urban level, which relies on the agglomeration of the energy requirements and the infrastructures for energetic conversion. This allows the designers to make the best decision, taking into consideration the district topology, the energy demands and the cost constraints.

The main variation of this method is about a different prospective, since differently to the other works available in the literature, it hasn't been evaluated a neighborhood keeping all the buildings connected to the DN, but a progressive set of networks' layout are generated based on a growing power coming from the centralized feeding system of the network. The centralized feeding system, or central plant (CP), is required for balancing the district network due to the lack of the working fluid in the prescribed phase. The selected technology for the central plant is based on the CO_2 as a working fluid and configured as an open cycle. The CP, during the summer mode, is composed just by a condenser, so when it is required CO_2 in the liquid phase. While, along the winter mode, the CP works as a proper heat pump. A full description is reported in the Appendix A.

The method is split into two branches, the first takes care of the network design and secondly the optimization of an energetic system, which in this case is defined as a superstructure of technologies. A key point is the distinction of the buildings in two different typologies, the buildings connected to the district network with heat pumps and the rest requires a standalone technology. The results of the two branches are then cross each other in order to take into consideration different options and looking for the optimum from a thermoeconomic point of view.

2.1 State of the art

The methods, regarding the DN energetic integration, available in the literature are usually split into two levels: individual building and urban scale. The lowest level of analysis is the individual building, since it covers the building design and further their renovation and maintenance [11]. This requires a highly accurate model, which usually leads to an important computation time. The highest level, the urban scale, relies on the agglomeration of the energy requirements and the infrastructures for delivering the services to the district with a model of the urban system [11].

In the literature a two optimization levels method for DH integration has already been exploited in the work of Lund et al. [12], which is focused on the optimization of the insulation of the pipes, due to the not negligible thermal losses of the fourth generation networks. A comparable method to the present is the [13], where, starting from a rough set of data, it is able to generate a Pareto graph of feasible solutions, with an heuristic random generation of network's configurations for the whole district [13]. The idea of reaching an optimum not connecting all the buildings within a neighborhood has been developed also in [14], where the author has chosen to generate different networks with the same layout, exploiting the energetic plant of some buildings. This solution doesn't allow to use a central plant, which is able to harvest heat from a natural resource, e.g. a lake or a river, one of the main characteristics of a district network.
von Rhein et al. compared the 5G with the previous generations of DNs, focusing also on the distinction between connected and not connected buildings to the network, but without integrating an advanced energetic model [15].

2.2 Definition of the method

The proposed method adopt a double optimization approach, as in fig. 2.1. The first optimization is about the construction of the network considering the available pathway, which is done by a MILP problem and solved by the solver CPLEX. The boundary conditions affecting the problem are the energy demand of the buildings, the starting point of the network and the topology of the roads, where the pipes are supposed to be placed. Furthermore a retrofitting of the network is studied, considering that some pipes are previously installed, so a null cost is assigned to those segments. A first design of the network adopts the extreme demand of the buildings, in order to accomplish the worst possible working condition. The network power bound is intended as the power provided by the CP and it allows the network to reach those buildings with an equal total amount of power demand. All this data are set up in an input file to feed the MILP problem. The following step is the post-processing, where it is refined the estimation of the cost of the network, since the cost function of the pipes and of the operating costs are non-linear. This entire process is looped by assuming the power provided to the network as a discrete

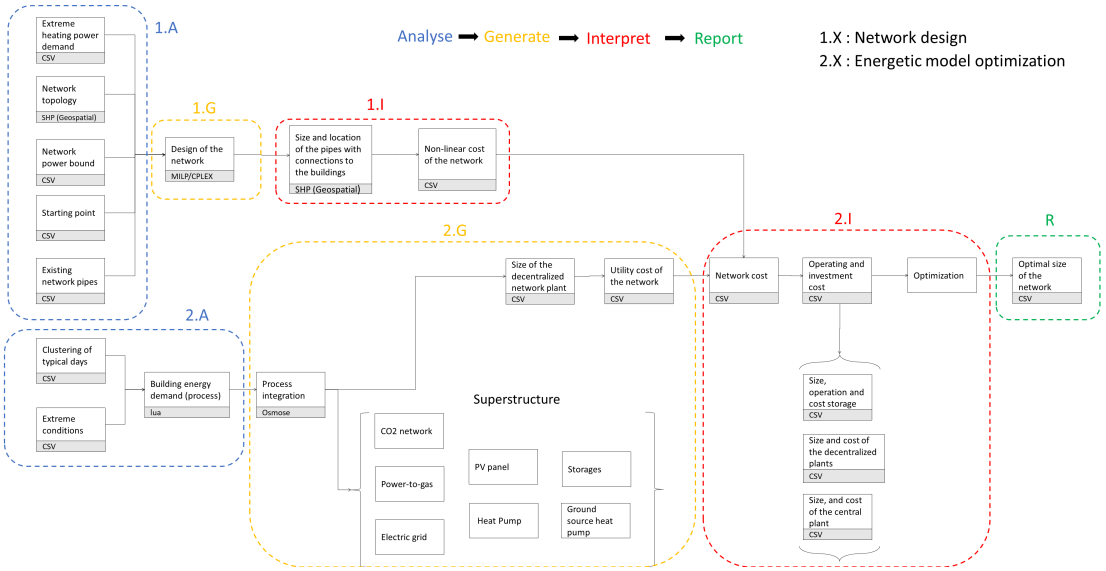

Figure 2.1: Flow chart of the methodology

variable, so it is possible to generate a growing layout of the network and distinguish a coverage ratio of the network through the neighborhood.

The second optimization takes care of integrating a superstructure of technologies to solve the heat cascade, the mass-energy balance and minimizing an objective function, while it covers the urban demand. The starting point is the clustering of the weather forecast into typical days and the report of the extreme, which is filtered out along the cluster process, but it is relevant for the sizing of the technologies. The next step is the integration of the model, which is a MILP problem, solved by Osmose, a software of IPESE's license. The superstructure includes PV panels, a central plant for providing CO_2 with the phase of liquid/vapour, a power-to-gas plant, a set of HPs for both the buildings connected or not to the DN and the systems of storages for all the resources available. This second optimization takes also into account the different amount of power assigned to the central plant, in order to distinguish the HPs that are exchanging heat with the network and those adopting instead a geothermal/air source. Moreover, it is developed a focus on the cooling system of a data center, which can bring a potential increasing of the energy savings by taking advantage of the waste heat recovery.

After solving the two branches the results are crossed for retrieving the specific total costs, in order to reach the minimum value.

3

Energy demand estimation

The integration of an energy system requires a model for the estimation of the buildings' energy demand, so in this section it has been explored a model to achieve a consistent analysis. The model is based on the weather forecast of Sion and the buildings' characteristics as input data, which leads to get the temperature profile of the buildings and the estimation of the hourly energy demand grouped by typology.
This work adopts the energy signature model, a linear regression technique, in combination with geodata, as previously done in the work of Girardin et al. [16]. Furthermore, the generation of a consistent model requires a classification of the buildings, which depends on the construction techniques and usage, since the thermal losses and comfort differ case by case.
Secondly the model is applied to the case study of this work, the requalification plan of neighborhood of Sion in Switzerland. The district is going to include 192 building for a total energy reference area of 583.407 m^2. The energy estimation results in a yearly energy demand split into single requirement, which in this case are a space heating of 30.296 MWh, a domestic hot water of 8.431 MWh, a cooling of 5.620 MWh, a refrigeration of 1.859 MWh and an amount of electricity equal to 14.347 MWh. The difference among the thermal requirements is the supply temperature, since for cooling is 20°C, for refrigeration is 12°C , for the domestic hot water is 55° and for the space heating is function of the external temperature. Moreover, it is computed the extreme heating demand in anticipation of the network design.

3.1 Energy signature model

Models for the estimation of the building's energy demand have been extensively developed in the literature.

The concept here exploited is based on the linear regression technique, which from a measurement campaign is able to predict the energy consumption with a 90% confidence level [17]. Furthermore statistical methods based on the energy signature have been introduced for estimating the heating and cooling demand [18]. A step even forward is achieved in [16] with the integration of a GIS (Geographic Information System) database. This brings an important advantage, giving information on the availability of endogenous resources (e.g.lake and surface water, underground water, geothermal heat) or waste heat available (e.g. data center or industries) [16].
The energy consumption measurements are highly time spending and the lack of results are widely diffuse, so the energy signature is applied for the estimation of the energy demand. The present estimation is based on the work of Girardin et al. [16], where it is developed a model that relies on the outdoor temperature (T_{ext}), a building classification based on usage, the year of construction or renovation and the temperatures of the hydronic system as a function of the heat to be delivered. A simplification consists of the neglect of the available buildings' roof surface for the installation of PV or solar panels, but it is adopted a coefficient related to the buildings' footprint.
The estimation of the heating and cooling loads require, as input, the external temperature and two linear regression coefficients: K_1 and K_2 [16]. This shapes the model as linear.
The specific heating and cooling demand in kW/m^2 is formulated at eq.3.1, where the index v indicates if it is related either to heating or cooling mode and z is the type of building combined with its state, due to the year of construction or renovation.

$$q_{v,z} = K_{1,v} \cdot T_{ext,z} + k_{2,v} \tag{3.1}$$

For the two linear regression coefficients are necessary the specific heating and cooling demands for a typical building, as close as possible to the one in evaluation in terms of conditions, since real measurements or energy bills aren't available. Furthermore, for taking into consideration the weather forecast, the number of heating and cooling degree days are defined, which consist of the difference between the external temperature and the threshold temperatures ($T_{th,v}$) multiplied for the selected time steps [19].

$$K_{1,v} = \frac{q_v}{dd} \tag{3.2}$$

$$K_{2,v} = -K_{1,v} \cdot T_{th,v} \tag{3.3}$$

3.2 District heat distribution system

The concept of the district network has, as the main parameters, the temperatures of supply and return of the working fluid, so a quick review is given for clarification of the process. It is assumed that the

supply temperature is given and the heat loads ($\dot{Q}_{n_k+1} - \dot{Q}_k$) are retrieved by the composite curve, where k indicates the intervals of temperature. So, the minimum flow rate, for the system, is computed with the eq.3.4, which is retrieved by getting the maximum between the minimum allowed return temperature ($T^{DHN}_{return,min}$) and the temperatures of the composite curve segments plus the minimum temperature difference (ΔT_{min}).
Otherwise, the return temperature is provided with the eq.3.5, where the supply temperature, the heat loads and mass flow rate are given.

$$\dot{m}_{DHN} = \max_{k=1,\dots,n_k} \frac{\dot{Q}_{n_k+1} - \dot{Q}_k}{c_p(T^{DHN}_{supply} - T')} \quad with \quad T' = max(T^{DHN}_{return,min}, T_k + \Delta T_{min}) \tag{3.4}$$

$$T^{DHN}_{return} = T^{DHN}_{supply} - \frac{\dot{Q}(T^{DHN}_{supply})}{\dot{m}^{DHN} \cdot c_p} \tag{3.5}$$

The heat exchanger area (eq.3.6) is obtained by summing, for each enthalpy interval ($\Delta\dot{Q}_k = \dot{Q}_{k+1} - \dot{Q}_k$), the heat-exchange matches between the network and the requirements composite curve of the buildings [20].

$$A^{DHN,hx} = \sum_{i=1}^{n_k} A_k = \sum_{i=1}^{n_k} \frac{\dot{Q}_k}{U_k \cdot \Delta T_{ln,k}} \tag{3.6}$$

The global heat exchange coefficient (U_k $[W/(m \cdot K)]$) is taken by the specific case of the two side of the heat exchanger. The distribution of the heat to the buildings requires the estimation of the heat exchanger area (m^2) for each of them, that is proportional to their marginal contribution at the nominal load ($\dot{Q}_{b,0}$) to the total demand [20] as in eq.3.7.

$$A^{DHN,hx}_b = \frac{\dot{Q}_{b,0}}{\sum_b \dot{Q}_{b,0}} \cdot A^{DHN,hx} \tag{3.7}$$

3.3 Energy demand Ronquoz

This work is based on the requalification of Ronquoz, a district in Sion (Switzerland). The area will face an important transformation in the following years, as described in the municipal report of the city of Sion [21]. The buildings have a mixed affections, quantifiable in term of energy reference area (ERA) as 37% of residential, 55% of office and 8% of commercial, with a total amout of ERA equal to 583.407 m^2. The estimated population is not reported and it will not be taken into consideration, since the ERA is enough for an estimation of the energy demand. Due to the lack of the measurements' energy demand is retrieved with the energy signature model, as previously described.

3.3.1 Buildings' estimation

In the report [21] the district is split in sectors, as we can see in the Fig.3.1 and a broad mix of typologies for the buildings are specified:

- Commercial
- Residential
- Industrial

Figure 3.1: Sectors Ronquoz

For each sector and subsector is given the IUS (heated surface) and IBUS (total surface), mandatory for the estimation of the energy demand. In particular is taken the heated surface for the estimation (Table 3.1). Furthermore for each category of the building is necessary to retrieve the thermal energy services, that for this work are:

- Space heating
- Air conditioning
- Hot water preparation
- Refrigeration

Hence, they covered the macro typologies of the buildings provided by the requalification plan, and to the thermal energy services join the electrical demand. In addition, since the district is going to face an important changes for the old buildings left out of the upgrade, a renovation is supposed, to reach the same performance in terms of heat losses as the new buildings.
A downside of this method is that the energy demands present sudden jumps due to the temperature of thresholds, one referenced to heating and another for cooling, respectively 15.7°C and 18°C for this case.
For a better understanding of the case study the plot of the external temperature (Fig. 5.1) over which is the most important variable since influence every sort of energy demand. The winter is prevalent, so the heating demand will be more relevant from the energy point of view.

Sector	Sub-sector	Heated surface [m^2]	Residential [%]	General [%]	Commercial [%]
A	A1	9905	0	81	19
	A2	37381	29	71	0
	A3	28388	42	50	7
	A4	31373	0	97	2
B	B1	19986	43	48	9
	B2	26060	54	46	1
	B3	74755	25	74	1
C	C1	0	0	100	0
	C2	0	100	0	0
	C3	27952	42	51	7
D	D1	18602	89	10	1
	D2	34264	33	29	38
E	E1	5764	0	71	29
	E2	0	0	100	0
	E3	6680	0	100	0
	E4	1995	0	61	39
F	F1	4200	0	100	0
	F2	37877	58	33	9
	F3	17300	17	76	7
	F4	16470	89	0	11
G	G1	23364	43	46	11
	G2	26128	84	0	16
	G3	8231	84	0	16
H	H1	10521	0	100	0
	H2	62026	7	89	4
	H3	36731	47	48	4
	H4	17454	85	4	11
	H5	0	0	0	0

Table 3.1: District specifics

Building type		Residential	Commercial	Industrial
q_{sh}	[kWh/m^2]	56.3	46.4	46.7
q_{dhw}	[kWh/m^2]	22.2	6.1	7.0
q_{ac}	[kWh/m^2]	0.0	25.37	0.0
q_{ref}	[kWh/m^2]	0.0	6.35	6.35
elec	[kWh/m^2]	27.78	22.22	16.67
HDD	-	62010	62010	62010
CDD	-	8210	8210	8210
$T_{th,heating}$	[°C]	15.7	15.7	15.7
$T_{th,cooling}$	[°C]	18.0	18.0	18.0

Table 3.2: Yearly energy requirement

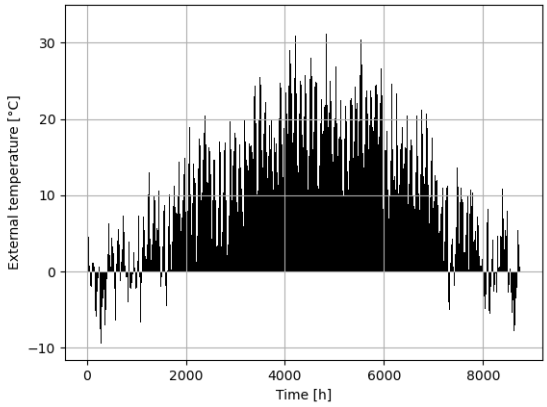

Figure 3.2: Yearly external temperature

3.3.2 Composite Curve of the district

The composite curves represent graphically the sum of the streams defined by temperatures and heat flow, which relies on solving the heat cascade of the process. In this section is interesting to display the composite curves of the cooling and heating demand of the neighborhood. So, two example are in fig.3.3 and fig.3.4, respectively for the second and third typical day, which concept is developed at the *Section 5.1*. In these plots the heating demand is referred as the cold streams and the cooling demand is the hot streams, since they are retrieved from the power plants point of view.

3.3.3 Heating and cooling energy map

The energy map is the result of the previous estimation. From the requalification plan are retrieved the typologies of buildings, which is particularly precise, considering also the single floors are differentiated.

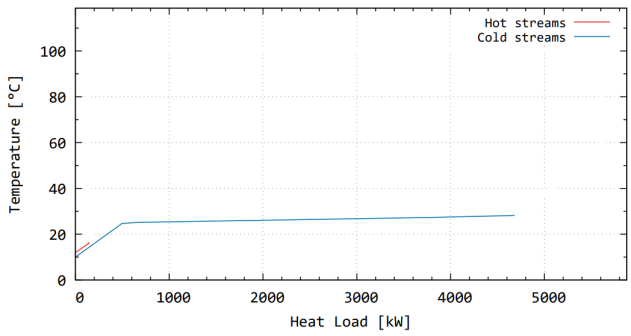

Figure 3.3: Composite curve of the heat demand for the second typical day

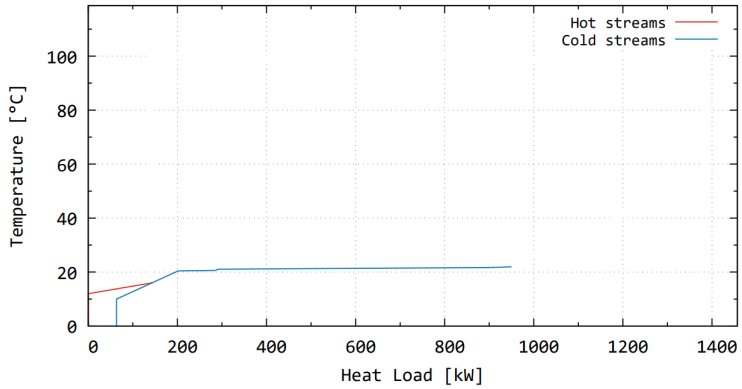

Figure 3.4: Composite curve of the heat demand for the third typical day

In the fig. 3.5 is plotted the yearly heating demand, summing up the space heating and the domestic hot water. And in the fig. 3.6 the yearly demand for air cooling and refrigeration.

This is the first step for identifying the most critical buildings, since they will influence the construction of the district network.

The identification of the most important consumers helps the designer to choose the starting point of the network, a crucial parameter for the effectiveness of the system. In this specific case the 20% of the most critical buildings requires the 37.5%, as in Fig. 3.7, so there isn't a significant impact of those buildings.

3.3.4 Extreme heating demand

In anticipation of the design of the district network, it is necessary to perform the energy demand from the network point of view. The design requires to retrieve the extreme conditions, since the demand

Figure 3.5: Energy heating map

Figure 3.6: Energy cooling map

must be satisfied in every time step of the model, hence the worst case scenario is during the winter when the external temperature reaches -9.2°C.
The required parameter to define the amount of heat, keeping the DN as a heat source, is the coefficient of performance (COP) with the eq.3.8 in the case of HPs for space heating and domestic hot water. The components of the equation are the temperature of condensation (T_{cond}), the temperature of evaporation (T_{evap}) and the total Carnot efficiency (η_{carnot}).

$$COP_{SH,DHW} = \frac{T_{cond}}{T_{cond} - T_{evap}} \cdot \eta_{carnot} \tag{3.8}$$

The extreme condition has two heat demands, the first for space heating and the second for domestic heat water, with a respectively COP of 10.76 and 4.92.

The data about the peak energy demand of the neighborhood is in Table 3.3, where the *demand* is in kW and *Id* is the identification code of the building.

Id	demand	Id	demand	Id	demand	Id	demand
B1001	53.72	B1049	88.68	B1097	86.72	B1145	40.87
B1002	53.72	B1050	88.68	B1098	86.72	B1146	40.87
B1003	53.72	B1051	88.68	B1099	86.72	B1147	40.87
B1004	53.72	B1052	81.69	B1100	86.72	B1148	40.87
B1005	175.02	B1053	81.68	B1101	86.72	B1149	40.87
B1006	233.01	B1054	116.47	B1102	86.72	B1150	40.87
B1007	233.01	B1055	116.47	B1103	86.72	B1151	40.87
B1008	233.01	B1056	116.47	B1104	86.72	B1152	40.87
B1009	233.01	B1057	116.47	B1105	86.64	B1153	40.87
B1010	67.04	B1058	116.47	B1106	95.96	B1154	40.87
B1011	62.17	B1059	116.47	B1107	97.02	B1155	40.87
B1012	89.25	B1060	116.47	B1108	97.02	B1156	40.87
B1013	89.25	B1061	116.47	B1109	97.02	B1157	40.87
B1014	89.25	B1062	109.23	B1110	124.33	B1158	40.87
B1015	89.25	B1063	109.23	B1111	124.33	B1159	28.8
B1016	37.3	B1064	109.23	B1112	89.98	B1160	95.86
B1017	35.7	B1065	87.49	B1113	95.96	B1161	142.32
B1018	62.48	B1066	87.49	B1114	89.98	B1162	142.32
B1019	62.48	B1067	87.49	B1115	89.98	B1163	142.32
B1020	62.48	B1068	84.3	B1116	97.02	B1164	100.39
B1021	23.46	B1069	87.49	B1117	97.01	B1165	131.05
B1022	21.76	B1070	87.49	B1118	97.01	B1166	100.39
B1023	60.14	B1071	81.14	B1119	40.93	B1167	131.05
B1024	58.6	B1072	85.25	B1120	37.96	B1168	67.76
B1025	59.69	B1073	85.25	B1121	37.96	B1169	67.76
B1026	46.93	B1074	54.26	B1122	50.74	B1170	52.40
B1027	46.93	B1075	72.22	B1123	50.74	B1171	52.40
B1028	46.93	B1076	72.22	B1124	50.74	B1172	52.40
B1029	59.6	B1077	72.22	B1125	50.74	B1173	67.76
B1030	44.48	B1078	50.31	B1126	49.52	B1174	42.00
B1031	59.2	B1079	72.22	B1127	49.52	B1175	111.04
B1032	11.12	B1080	118.62	B1128	52.46	B1176	111.04
B1033	55.52	B1081	54.26	B1129	52.46	B1177	142.32
B1034	59.2	B1082	50.31	B1130	52.46	B1178	100.39
B1035	44.47	B1083	118.62	B1131	52.46	B1179	131.05
B1036	41.24	B1084	114.18	B1132	52.46	B1180	131.05
B1037	55.52	B1085	89.1	B1133	52.46	B1181	218.08

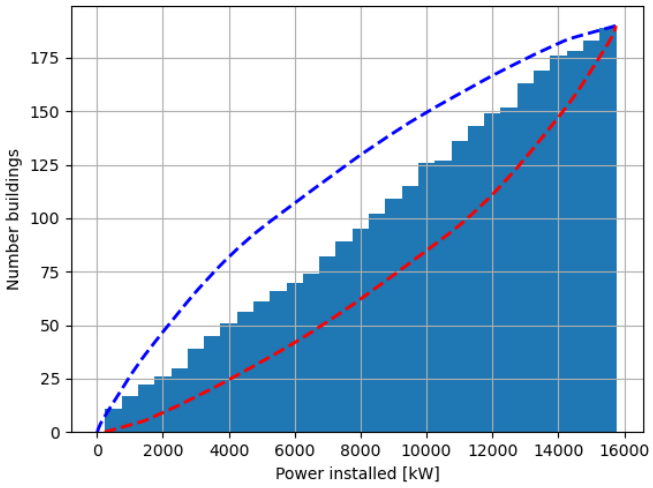

Figure 3.7: Power installed-number buildings

B1038	59.2	B1086	118.62	B1134	52.46	B1182	142.32
B1039	59.2	B1087	118.62	B1135	52.46	B1183	142.32
B1040	44.47	B1088	235.17	B1136	52.46	B1184	100.39
B1041	44.48	B1089	109.76	B1137	131.05	B1185	100.39
B1042	55.52	B1090	109.76	B1138	131.05	B1186	130.05
B1043	44.47	B1091	114.18	B1139	50.42	B1187	72.65
B1044	59.2	B1092	62.75	B1140	125.96	B1188	78.34
B1045	88.68	B1093	67.65	B1141	50.42	B1189	76.69
B1046	88.68	B1094	67.68	B1142	40.93	B1190	87.93
B1047	88.68	B1095	124.33	B1143	102.25	B1191	124.8
B1048	88.68	B1096	93.52	B1144	28.47	B1192	40.82

Table 3.3: Extreme energy condition for the network

4 Network design

The network has the task to link the buildings while keeping into consideration the energy demand and the layout of a suitable path for the pipes. The network is built as a tree and, thanks to a system of equations and an objective function, it is possible to set up a MILP problem. The aim is to achieve a minimization of the investment cost and ensuring that the total amount of the energy demand, about the buildings of the neighborhood, matches the power installed at the central plant.
In this chapter a methodology is developed to reach the maximum cost saving, e.g. performing multiple initial points of the network, keeping in place pre-existing pipes and considering a set of power installed at the centralized feeding plant. Furthermore, they are described all the steps involved to set and solve the MILP problem, starting from rough data.

4.1 State of the art

This section describes a literature review of the existing methods used for modelling and optimizing the district energy networks.
The main characteristic for defining the level of detail of the network design is the phase of planning, which can be described in three stages:

- Simulation and control: it covers a highly defined simulation and control of the network;
- Refined design: it includes the selection of the standard pipe sizes the insulation and the booster system for covering the pressure losses;
- Strategic design: it's necessary to verify the economic feasibility, so it is defined the network layout and the size of the power units;

In this work, the method is meant to provide an analysis of the strategic design, specifically about the design layout, the not-standard selection of the pipes and a rough evaluation of the operating costs for keeping the system at the working pressure.
In the literature, the design of a district network is explored in different ways, combining linear and non-linear models with deterministic and heuristic solution methods [22]. A non-linear model is necessary when the variables are described by non-linear functions, e.g. highly defined models of the fluid dynamic behaviour and constraining the system with a polynomial function regarding the cost of pipes [23]. These models are usually solved with heuristic methods, with the disadvantage of not leading to the optimal solution, but it could even be a good approach for infeasible large scale problems (e.g. network design optimization), since it would find all the near-optimal design [24].
For the purpose of this work is suitable a linear model for the optimization of the DN, so the problem is set as a mixed-integer linear programming (MILP), a combination of continuous and integer variables. Particularly, a deterministic method is more suitable for linear optimization, since it gives the huge advantage of finding the global optimal solution.
MILP problems are widely used in the optimization of district networks and in the literature are reported many examples, as in [25].
The remarkable work of Bordin et al. [25] includes a MILP method for the expansion of an existing DN to new possible users. An interesting part is the definition of the distribution and the connection cost, which has been target also in this work.
A method to analyse, in an early stage, the requirements of all the parties involved is in [26], where he integrates also a distributed energy system (DES) and he explains how to implement constraints about existing pipes and tanks in order to exploit all the possibilities. From the same author a focus on the economical evaluation of the heat exchangers is reported in [27], where it is also described the process for reaching a piecewise linear price function. Furthermore Haikarainen et al. developed a MILP model for optimizing also the storages of the district network, by keeping as a parameter the position of the storages, proving the flexibility and a certain degree of solvency of the linear models [28].
In the literature, there aren't many works including also geographic information system, but [29] is a great example of the potential of this data, since Baldvinsson et al. have been able to integrate a different energy system and reducing the working temperature of the district network, as it is done in this work for a 5G network.

4.2 Process for the network design

The process for the generation of the network is split into three steps as described in fig.4.1 and it will drive to a dataframe holding all the information about the DN.
The first aspect is the preparation of the input data, taken over by the pre-process, since rough data are

made available, so they contain duplicates and misleading values most of the time. For developing the pre-process is necessary a Geographic Information System (GIS) software for spatial data manipulation, QGIS in this case, for being able to visualize the shapefiles. This tool allows an easier approach to the geographical data and it has powerful illustrative options. Then, QGIS is matched with a script written in Python, an high level programming language, for manipulating the data and avoiding many tedious operations, otherwise done by hand.
After the first phase, it comes the key point of the whole process, the optimization. The system of equations for achieving the optimal solution is formulated thanks to AMPL (A Mathematical Programming Language) and Cplex as a solver, which is owned by IBM, but kept open source.
The final step is reached by presenting the results in a distinctly way, with the union of QGIS and Python for manipulating the data before the final presentation.

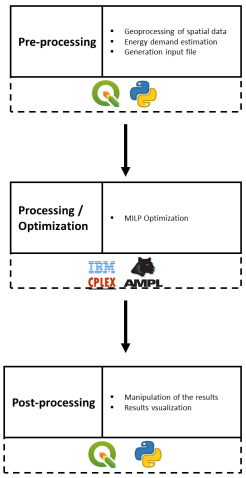

Figure 4.1: Method for the generation of the network

4.2.1 Geoprocessing

The geoprocessing is a crucial aspect of this work. The spatial data are taken from OpenStreetMap, therefore they must be cleaned, merged and simplified. This is as much tedious as important, even just one wrong element could bring completely misleading results.
The mathematical structure of the network consists of a graph made by nodes, coming from buildings and road intersections, and connected by edges. This structure is synthesized in a ".dat" file, with the numerical description of the position of nodes, the connection of the nodes and the heat demand.
A summary of a typical process is described hereafter:

- Cleaning of the layer containing the roads with QGIS;

- Construction of the buildings, representing them as polygons, of the district of Ronquoz based on the requalification plan. The it is approached the conversion of the polygons into points, taking the centroids of the buildings and the connection of them to the road thanks to the method of smallest eucledian distance;
- Assigning of the heating demand to the buildings and generation of the input file, which is automatized with a script in Python.

4.2.2 Optimization

Approaching the mathematical problem requires, firstly, to individuate the critical variables involved in the design of the district network, these are the layout of the potential pipes, their sections and the thermal requirements of the decentralized technology implemented in combination of the buildings. The section is kept as a continuous variable, even if in the market just predefined sizes are available, but this method is done for a first estimation of costs and these choices are usually taken just before the final commitment.
The optimization of the DN design is formulated in AMPL as a MILP (Mixed Integer Linear Programming), with as the objective function the minimization of the overall sum of the investment costs, depending on length and section of the pipes.
The input parameters cover both topological and thermodynamic properties. In the case of the topological properties, the nodes of the path of the graph are set with an incremental numeration, the absolute position and the power demand, which is settle equal to the power correspondent to the requirements decentralized technology for each building and zero for the rest, assuming the losses negligible at this stage. These nodes are connected by edges and for each couple of points is assumed to be allowed just one edge, which is characterized by a pipe for the liquid CO_2 and one for the vapour CO_2.
The thermal energy transferred along the network is achieved glad to the latent heat of the CO_2 near the saturation point in the vapour and liquid phase.
The temperatures of the network are 13°C and 15°C in the liquid CO_2 and vapour CO_2 for with a saturation pressure corresponding to 5.0 MPa, which guarantees 186.42 kJ/kg of latent heat for the condensation for a saturation temperature of 14.3°C. This level of pressure has been chosen in order to to stay in the saturation temperature range below 16°C, so the network can take advantage of the free air cooling, thanks to the gas expansion.
The pressure losses have a high impact on the district networks, because a change of phase could ruin the operation of the system. Therefore, a system of boosters are installed along the pipes [8]. The thermodynamic properties for the network are fully reported in the table 4.2. The velocities of vapour and liquid are kept constant along the DN, because the sections are very sensible on these factors and thus assuming the velocities as variable bring the model to be too complex [30] and it isn't a goal of this work

to analyze it. A bunch of assumptions are also necessary, in order to keep into consideration problems that may occur in the network, e.g. the cavitation occurring in the liquid pipes can be a cost factor due to the maintenance, so it is preferred to keep the condition as specified in [31]. An important aspect for setting the mathematical problem is the difference of enthalpy, but since the difference of the temperatures and pressures in both the pipes is supposed to be constant, the difference of enthalpy in every part of the network between the the liquid CO_2 and vapour CO_2 is assumed constant as well.

Δh_{CO_2}	[kJ/kg]	186.42
ρ_{liq}	$[kg/m^3]$	842.35
ρ_{vap}	$[kg/m^3]$	154.64
v_{liq}	[m/s]	3
v_{vap}	[m/s]	4

Table 4.1: Thermodynamic properties for the network

4.2.3 MILP FORMULATION

In this section is explained the mathematical formulation for the generation of the network, which adopts a MILP problem in order to build and optimize the pipes system. The MILP problem involves both discrete and continuous variables, and the optimization object is set to minimize the investment cost, respecting the energy balance along the network. The investment cost function (eq.4.1) is retrieved by a linearization of a given function, that is not possible to disclose.

$$IC = \sum_{i,j \in pipes} (Cost_1 \cdot (Section_{liq\,i,j} + Section_{vap\,i,j}) \cdot L_{i,j} + Cost_2 \cdot L_{i,j}) \tag{4.1}$$

Two types of constrains are bounding the problem, the topological map of the district and the power balance along the network.
The topological constraints are necessary to build the graph inside the MILP problem. The concept is based on creating a tree graph, that means just one edge is allowed for joining two specific vertices, thus it can be defined as an undirected acyclic graph, so basically a disjoint union of trees.
After this small preview, it is possible to describe the investment cost function (eq.4.1). The variables of the investment cost are the sections of the pipes and the lengths of the edges, while the $Cost_1$ and $Cost_2$ are constants and carried out by the linearization of the non-linear cost function. From now on is possible to describe the MILP problem, considering that the path is characterized by the indexes, going from the node i toward the j. The first set of equations is the topological constraints, in order to consider the

available path.

$$\sum_{s} X_s = 1 \quad \forall \quad X_s \quad binary \qquad s \in StartNodes \tag{4.2}$$

$$\sum_{s,i} Y_{s,i} \geq 1 \quad \forall \quad Y_{s,i} \quad binary \qquad s,i \in pipes, \quad s \in StartNodes \tag{4.3}$$

$$\sum_{i,s} Y_{i,s} = 0 \quad \forall \quad Y_{i,s} \quad binary \qquad i,s \in pipes, \quad s \in StartNodes \tag{4.4}$$

$$\sum_{s1,s2} Y_{s1,s2} = 0 \quad \forall \quad Y_{s1,s2} \quad binary \qquad s1,s2 \in pipes, \quad s1,s2 \in StartNodes \tag{4.5}$$

$$Y_{j,n} = X_j \quad \forall \quad Y_{j,n} \quad binary, \quad X_j \quad binary \qquad j,n \in pipes \tag{4.6}$$

$$\sum_{j,n} Y_{j,n} = X_n \quad \forall \quad Y_{j,n} \quad binary, \quad X_n \quad binary \qquad j,n \in pipes \tag{4.7}$$

$$Y_{j,n} + Y_{n,j} \leq 1 \quad \forall \quad Y_{j,n} \quad binary, \quad Y_{n,j} \quad binary \qquad j,n \in pipes \tag{4.8}$$

About the binaries, they are equal to 1 if the node X_i or the edge Y_{ij} is selected, otherwise they are set to 0. Furthermore, describing downward, the node s is the starting point of the graph (eq.4.2), which is automatically set up as activated.The starting point is imposed in the input file and it is basically chosen by the designer. This node is allowed to be reached at least by one edge, thanks to the eq.4.3, and it isn't allowed to the graph to come back (4.4). The eq.4.5 forbids to rejoin the trees, so the definition of tree graph is satisfied.
The growth of the graph is given by the eq.4.6, the eq.4.7 and eq.4.8. These three equations impose respectively to generate a set of connected nodes, to have the number of edges equal to the number of activations of a certain node and to constrain the edges to avoid any way back.
The second set of equation is due to the energy bound, that allows to set the power installed at the centralized feeding system, by assigning the value M (eq.4.9), where $P_{dim,n}$ is the power demand at the node (n). M is assumed as a discrete variable, in order to retrieve a progressive expansion of the network

through the neighborhood.

$$\sum_{n} X_n \cdot P_{dim,n} \geq M \quad \forall \quad n \in nodes \tag{4.9}$$

Other than satisfying just the topological constraints, the problem must face the flow balance, that is respected at each node. In this case, the flow balance is converted as a power balance, in order to simplify the problem (eq.4.10).

$$\sum_{j,n} Trans_{j,n} = P_{dim,n} \cdot X_n + \sum_{n,i} Trans_{n,i} \quad \forall \quad j,n \in pipes, \quad n,i \in pipes \tag{4.10}$$

The *Trans* is the quantity of heat transferred between two nodes. And it is required another equation to guarantee that the transferred heat is equal to the one prescribed by the input file for the sum of the activated nodes (eq.4.11).

$$\sum_{s,n} Trans_{s,n} = \sum_{n} P_{dim,n} \cdot X_n \quad \forall \quad s,n \in pipes \notin StartNodes \quad n \in nodes \notin StartNodes \tag{4.11}$$

Moreover, it is necessary to defined also the power that a certain section of the pipe is able to transfer, which is correlated to the thermodynamic properties of the CO_2 and the power balance at the nodes (eq.4.12 and eq.4.13). The minimum power to transfer is equal to the lowest node requirements of the network (eq.4.15) and the maximum power is the sum of all the nodes requirements (4.14), which corresponds to the main pipes of the network.

$$Trans_{j,n} \leq Debit_{max} \cdot Y_{j,n} \quad \forall \quad Y_{j,n} \quad binary, \qquad j,n \in pipes \tag{4.12}$$

$$Trans_{j,n} \geq Debit_{min} \cdot Y_{j,n} \quad \forall \quad Y_{j,n} \quad binary, \qquad j,n \in pipes \tag{4.13}$$

$$Debit_{max} = \sum_{n \in nodes} P_{dim,n} \tag{4.14}$$

$$Debit_{min} = \min_{n \in nodes} P_{dim,n} \tag{4.15}$$

The last step is to convert the power transferred to their pipe sections for the objective function. For this purpose are required the eq.4.16 and the eq.4.17.

$$Sec_{liq,ij} = \frac{Trans_{ij}}{\rho_{liq} \cdot v_{liq} \cdot h_{liq-vap}} \quad \forall \quad i,j \in pipes \tag{4.16}$$

$$Sec_{vap,ij} = \frac{Trans_{ij}}{\rho_{vap} \cdot v_{vap} \cdot h_{liq-vap}} \quad \forall \quad i,j \in pipes \tag{4.17}$$

It has been added to the model also a set of equations that take into account the possibility of evaluating the existing account, which is described in one of the following sections.

4.2.4 Post-processing

As soon as the results of the optimization are available, a visualization of the design is plot on QGIS, which allows to verify the consistency of the optimization. The final step of the evaluation of the design of a DN is from the economical point of view. The two variables to study are the investment and the operating cost, which is evaluated by taking into account just the pressure losses and the following implementation of boosting system, for keeping the pressure at the operating level and avoiding phase transition, since it wouldn't assure to deliver the proper amount of thermal energy. The operating cost is formulated at the eq.4.18, which keeps into consideration the cost of the electricity ($Cost_{el}$), the amount of electrical energy (E_{pump}) and the efficiency of the boosters (η_{pump}). The eq.4.19 describes the electricity to provide for keeping the system at the right pressure, function of the pressure losses (ΔP) and differentiating the thermodynamic properties for the two phases.

$$OC_{yearly} = Cost_{el} \cdot E_{pump}/\eta_{pump} \tag{4.18}$$

$$E_{pump} = \sum \Delta P_{CO_2,liq,max} \cdot \dot{m}_{CO_2,\,liq}/\rho_{CO_2,liq} + \Delta P_{CO_2,vap,max} \cdot \dot{m}_{CO_2,vap}/\rho_{CO_2,vap} \tag{4.19}$$

Since with this formulation is retrieved the yearly operating cost, therefore also the investment cost is defined yearly (eq.4.20), so it is required an interest rate (i) and the lifetime of the plant (n), that is imposed equal to the one of the energetic system. The interest rate is set as 0.08, while the lifetime of the plant is equal to 20 years.

$$IC_{yearly} = IC_{tot} \frac{i \cdot (1+i)^n}{(1+i)^{(n-1)}} \tag{4.20}$$

In the post-process has been developed a linearization of the pressure losses to have a first estimation of the pressure losses. Hence they are implemented two equations, one for liquid (eq.4.21) and another for vapour (eq.4.22) drops.

$$P_{lossliq,ij} = (c_1 \cdot \sqrt{(4 \cdot Sec_{liq,ij}/\pi + c_2}) \cdot L_{i,j} \tag{4.21}$$

$$P_{lossvap,ij} = (c_3 \cdot \sqrt{(4 \cdot Sec_{vap,ij}/\pi) + c_4}) \cdot L_{i,j} \tag{4.22}$$

In a following step, the pressure drops of the pipes flow is evaluated adopting the Darcy-Weisbach equation [32](eq. 4.23), deeply more precise than the linear formulation, since the pressure loss is highly non-linear. Regarding the eq.4.23, the density is set at 842.35 kg/m^3 for the liquid phase and 154.64 kg/m^3 the vapour phase at 50 bar .

$$\Delta P = f\frac{L \cdot \rho \cdot V^2}{2 \cdot D} \tag{4.23}$$

where:
Δp pressure loss [Pa]
f is the the Darcy friction factor [-]
L is the length of pipe [m]
D is the diameter of pipe [m]
ρ is the density of fluid [kg/m^3]
V is the flow velocity [m/s]

And for the Darcy friction factor (f) has been used the formulation of Colebrook-White [33](eq. 4.24), where the surface roughness is imposed at 25 μm.

$$\frac{1}{\sqrt{f}} = -2log(\frac{e/D}{3.7} + \frac{2.51}{Re\sqrt{f}}) \tag{4.24}$$

where:
e is the roughness of the pipe [mm]
D is the diameter of pipe [m]
Re is the Reynolds number [-]

4.3 Expansion of the network

In this section, the expansion of the network takes place. To develop this aspect is imposed the growth of the power provided from the central plant to the network, in order to retrieved a set of different networks. The variables involved are the layout of the hypothetical pipes, the sections and the power capacity of the central plant itself, which is the parameter M in the system of equations of the previously section, while they are kept the same assumptions as well.
This approach is meant to solve the particularity of defining the optimal layout of a district network within a neighborhood, and considering the amount of energy completely centralized to take a thermal advantage on a specific natural source, e.g. lake and geothermal sources.
The first rough design of the network requires the estimation of the thermal energy demand, particularly

in this phase of the work is adopted the extreme condition, so when the energy requirement reaches its peak. Thus, the capacity of the pipes must be sufficient to handle the maximum amount of flow over the time steps. This is bringing an oversizing of the sections and an increment of the investment cost, but as a first computation is verified to be enough precise and estimating the reduction of flow rate due to the installation of the CO_2 tanks go beyond the purpose of this work.

Following the process here described, to generate a set of networks, will bring to define an optimal interval, or more than one, where the rate of cost and power installed is minimized. This segment will be set in the energetic model, in order to target the most promising configurations. In this way a lot of computation time is saved, since we are constraining the possible configurations of the energetic model. The results of the present formulation are plot in fig. 4.2 and fig. 4.2 respectively for liquid and vapour pipes. The growth of the network is achieved by improving the power of centralized feeding system, that is defined as a percentage over the total amount for covering the whole neighborhood, which is defined as coverage ratio. The nominal power for covering the whole neighborhood (coverage ratio of 100%) is 15.8 MW, and in the table is reported the progressive growth of the network, with different network factors.

Network factor	Nominal power [MW]
40%	6.3
50%	7.9
60%	9.5
70%	11.1
80%	12.7
90%	14.3
100%	15.8

Table 4.2: Thermodynamic properties for the network

4.4 Energetic considerations

A detailed numerical problem of the behaviour of the network requires the calculation of the local pressure and temperature of the CO_2 in the whole system of pipes. In fact, these are mandatory to determine the total amount of compression to keep the system working properly and due to the low temperature network the temperature losses are neglected.
As claimed before regarding the design of the sections of the pipes, the network design is based on the extreme conditions, but another approach could be studying the model for each time step evaluating as well the position of the storage tanks, avoiding an oversizing of the network, but this aspect go beyond the purpose of this work.

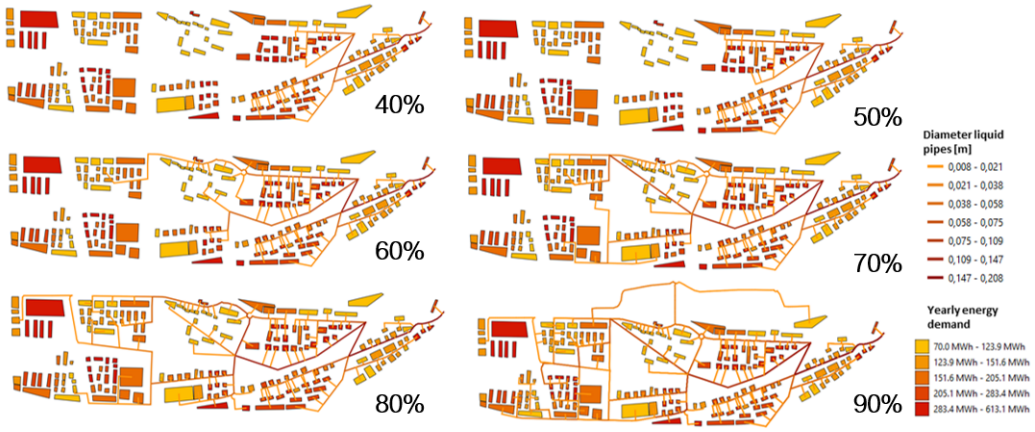

Figure 4.2: Expansion liquid DN

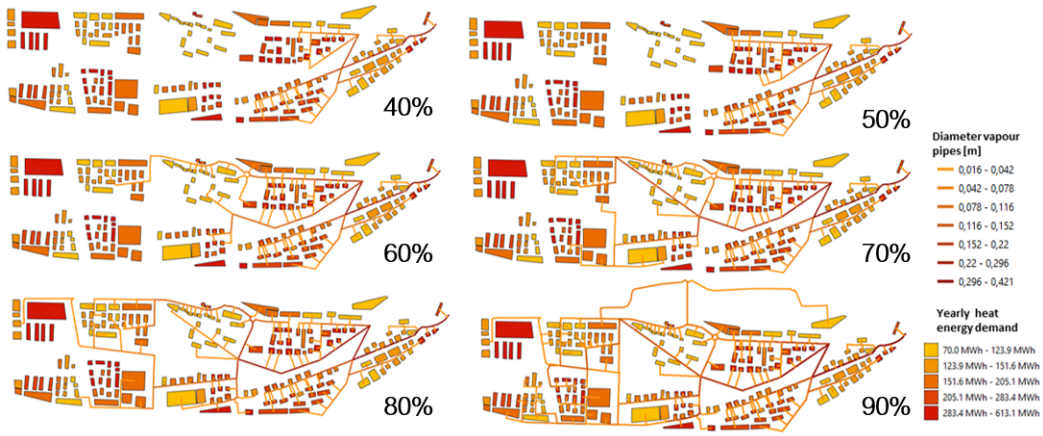

Figure 4.3: Expansion vapour DN

The difference of geodetic levels are negligible and therefore is not accounted for the losses calculation, this is due to a lack of accuracy of the geodata.

4.5 Starting point

The starting point of the network is influenced by the position of the central plant, which in turn is constrained by the availability of natural energy sources and by the position and demand of the buildings within the district. Hence, the starting point can be moved to a different node and recomputing another set of configurations for the networks. In this specific case is set up to three starting points, due the possible allocations of the central plant in the district of Ronquoz, as pointed in figure 4.4.

The results are plotted, in Fig.4.5, as the sum of the yearly investment and operating cost per m^2 of

Figure 4.4: Starting nodes of the network

ERA, about the connected buildings, for each starting point and power provided by the central plant. As it is possible to observe there is an interval of minimum from 4 MW to 8 MW for the first starting point, while the second has two segments characterized by a minimum, from 4 MW to 8 MW and another less important from 8 MW to 11 MW.

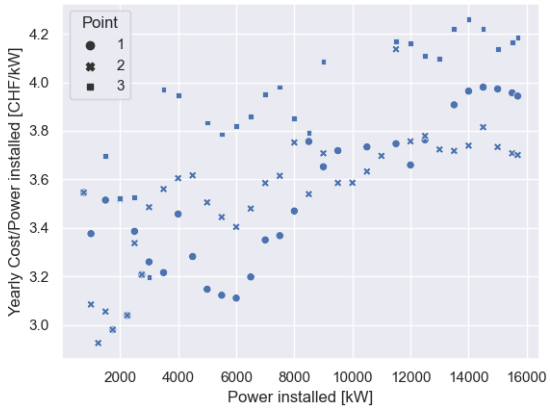

Figure 4.5: Cost pipe power installed

At low installed power the parameters are highly sensible to the position of the closest buildings, so there is a high fluctuation. Furthermore, the implementation of the starting points is meant for retrieving the minimum cost for a chosen amount of power installed. Hence, this concept is useful when applied in the context that is developed in this work, since it is based on the generation of a set of solutions for reaching the best economical solutions.

4.6 Implementation of a data center

Within this work is also integrated a data center for pursuing the waste heat recovery, so in this section is added another building in the neighborhood.
The position of the data center is supposedly chosen at the center of the map, since there aren't indi-

cations about this topic on the provided report. And besides, the heat dissipation of the server is estimated to result in 450 kW, on the network's side. The new set of results, following the same process as in the previously section, is plot in fig. 4.6, while is kept the starting point of the graph at the first point. The network covering the whole district is represented in fig.4.7 and fig.4.8, respectively for liquid and vapour pipes. The connection of the district network to the data center occurs from an installed capacity of 12 MW and up. So in this interval, it is realized an average saving of the 3.3%, regarding the ratio between yearly cost and power installed and compared with the configuration without the data center. This is due to the fact that the data center has been profitably placed at the center of the neighborhood.

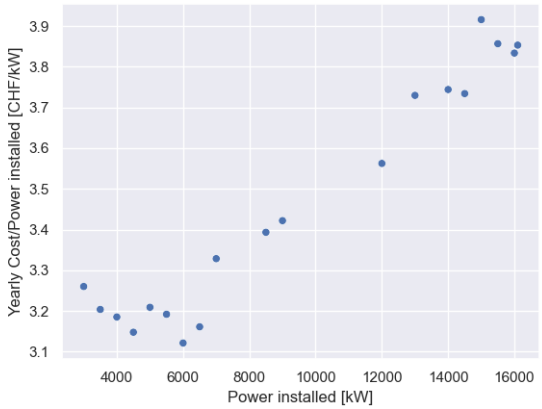

Figure 4.6: Cost pipe power installed Data Center

Figure 4.7: District design with the data center (liquid)

4.7 Existing pipes

The construction of the network requires a dual approach, the first avoiding any sort of constraint and the second facing up the previous implementation of some pipes, which are effectively already installed

Figure 4.8: District design with the data center (vapour)

in a part of the district. In order to take into consideration an existing implementation is set up as boundary constraints the maximum flow rate for those edges of the graph. Thus, the MILP problem has a new set of equations, in order to limit maximum flow rate for certain pipes.
The construction of the network begins from a set of raw spatial data, which after the manipulation is converted into the input data of the algorithm, capable of carrying out the graph. So, it requires to append among the input data also the existing pipes and their sections for constraining the flow rate, which is typically done manually.
The MILP formulation gets some new equation for integrating the new input data as following. Firstly, the equations of the sections of the pipes is modified in order to exclude the existing pipes:

$$Sec_{liq,ij} \geq \frac{Trans_{ij}}{\rho_{liq} \cdot v_{liq} \cdot h_{liq-vap}} \quad \forall \quad i,j \in pipes, \quad i,j \notin existing\ pipes$$

$$Sec_{vap,ij} \geq \frac{Trans_{ij}}{\rho_{vap} \cdot v_{vap} \cdot h_{liq-vap}} \quad \forall \quad i,j \in pipes, \quad i,j \notin existing\ pipes$$

Then, two equations for limiting the quantity of heat transported along the existing pipes are approached. in this way after that those pipes reach their limits another path is chosen by the system to fill the energy requirements:

$$Trans_{ij} \leq \rho_{liq} \cdot v_{liq} \cdot h_{liq-vap} \cdot Sec_{liq,ij} \quad \forall \quad i,j \in existing\ pipes$$

$$Trans_{ij} \leq \rho_{vap} \cdot v_{vap} \cdot h_{liq-vap} \cdot Sec_{vap,ij} \quad \forall \quad i,j \in existing\ pipes$$

So, in these segments the decision variables are the node X_i and the edge Y_{ij}, which are explained at the Section 4.2.3 . While, as objective function is kept the eq.4.1.

The consequent results about the case study is at the fig. 4.9, keeping just the first starting point. The new pipes are chocked at a power installed above 8000 kW, so the network add an alternative path for reaching the rest of the buildings. This aspect is clearly case dependent and this must be taken just as an example, without pretending to give an absolute answer whether is proper to keep the existing pipe or proceed with a brand new installation.

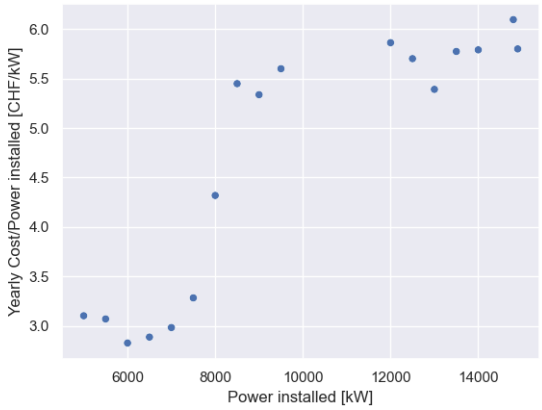

Figure 4.9: Cost pipe power installed with existing pipes

5 Energetic model

The energetic model is developed based on the implementation of the CO_2 district network, to exploit the exchange of energy among different technologies and buildings. The first step is the identification of the typical days of the city of Sion, to reduce the effort on the simulation, while keeping the results with a reduced error. In this section, after retrieving the energy demand are implemented two superstructure characterized by a power to gas for taking advantage of the excess of electricity, generated by the PV panels, to store methane for covering shorter periods of electricity and heat. Another challenging source of waste heat is also reviewed; a data center. This last integration is approached with a literature review for targeting the most suitable technology about a 5G district network. Furthermore a model is also dedicated to the economical feasibility of connecting the data center instead of exchanging heat with the surrounding atmosphere.

5.1 Clustering typical days

In order to decrease the computation time, the available data has been clustered using the k-medoids. From an estimation based on the silhouette coefficient an estimation of 8 typical days will applied to the model. Since the pure partition of the days is not precise, it is assigned a weight value, which represents the accuracy of the day itself. In other words, the weight of each typical day is the total amount of objects within the same cluster. It also must kept into consideration that this approach completely filter out the extreme energy demand, so causing an underestimation of the size about the storages.
The space heating demand is the clustering parameter since it is the main energy demand. The eight clusters of the typical days matched with the yearly weather forecast at the fig. 5.1 and the weight values are summarized at the Table 5.1.

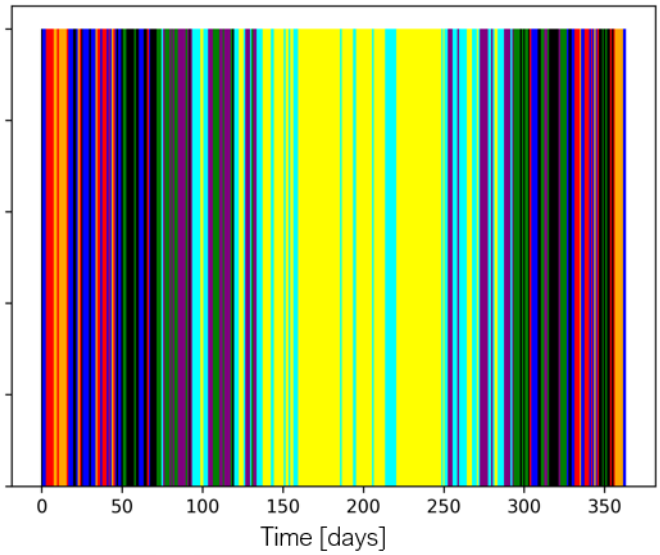

Figure 5.1: Yearly external temperature

-	1	2	3	4	5	6	7	8
Days	264	59	222	72	206	7	254	169
Weight	54	46	17	49	52	68	49	30

Table 5.1: Typical days

After retrieving the typical days, it is proper to plot them in order to have a full control of the model and avoiding misleading results, as it has been done in the following figures (fig.5.2, fig.5.3, fig.5.4).

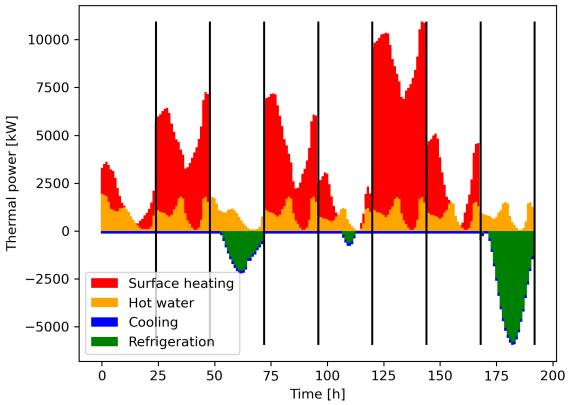

Figure 5.2: Thermal power of the typical days

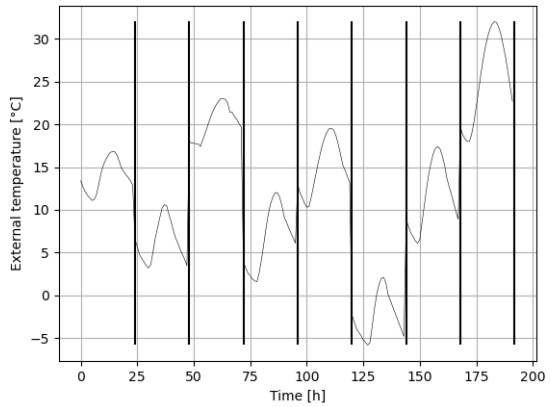

Figure 5.3: External temperature of the typical days

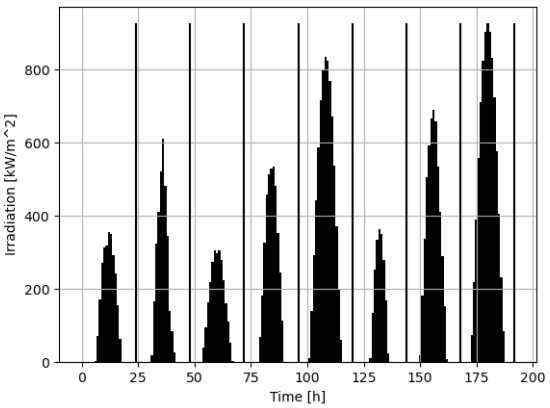

Figure 5.4: Solar irradiation of the typical days

5.1.1 K-Medoids

In this section, it has been justified the choice regarding the algorithm of clustering. The main two approaches widely used are the k-mean and k-medoids, so the first consideration is the k-means clustering is sensitive to outliers and since an object with an extremely high value may substantially distort the distribution of the data. Moving to k-medoids allows instead of taking mean of cluster we take the most centrally located point in cluster as it's center.
The dataset has 365 objects with one variable, the objects are assigned into 8 clusters. Thus, the k-medoids is based on the selection of the medoids m_p, which minimize the sum of the distances with

the other objects X_n within the cluster k objects, as in eq.5.1.

$$m_p = \min_{p \in K} \sum_{j=1}^{n} d(x_n, m_p) \quad with \quad p = 1, 2, 3, ..., k \tag{5.1}$$

5.1.2 Silhouette

The silhouette score is a measure of the similarity of an object to its own cluster in relation to other clusters. The number of clusters affects the quality of the clustering, so the silhouette score is a measure to evaluate such parameter and it is computed using the distances of the center of the cluster to other points of its group and the others. K is defined as the clusters' number and the Silhouette score is split into different levels. The score of each point is formulated at eq.5.2, which must be summed up with the points of the same cluster, as in eq.5.3. The last step is computing the average value by considering all the clusters, with the eq.5.4 [34].

$$S_{x(i)} = \frac{b_{x(i)} - a_{x(i)}}{max(a_{x(i)}, b_{x(i)})}$$

(5.2)

where:
$x(i)$ is the data point of the cluster , i =1,2,3,..., n.
$a_{x(i)}$ is average distance between x_i and every data point in the same cluster.
$b_{x(i)}$ is the minimum average distance between x_i and every data point in the other clusters.

$$S_k = \frac{\sum_{i=1}^{n} S_{x(i)}}{n} \tag{5.3}$$

where:
n is the number of data points in the same cluster.
$x(i)$ is the average distance between x_i and every data point in the same cluster.
$b_{x(i)}$ is the minimum average distance between x_i and every data point in the other clusters.

$$S_{avg} = \frac{\sum_{k=1}^{m} S_k}{m} \tag{5.4}$$

where:
m is the number of all clusters.

In the case of the clustering for the typical days, it is reached a maximum Silhouette score with eight clusters, as it is shown in the fig.5.5. So the decision to use 8 clusters for typical days is justified.

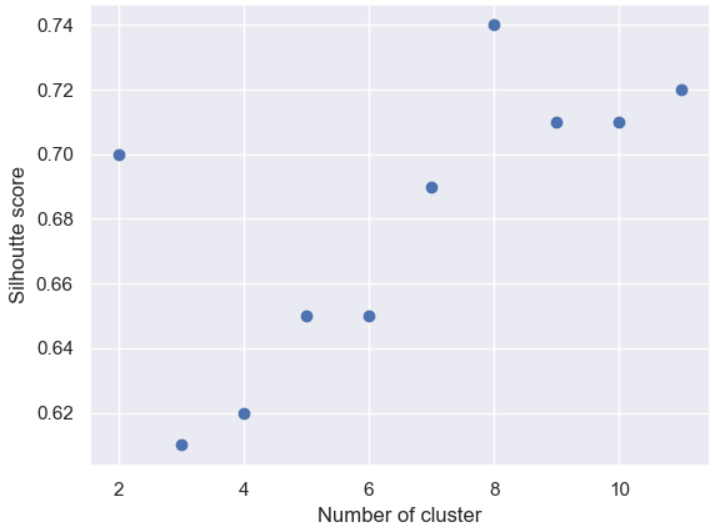

Figure 5.5: Silhouette score for the typical days' clustering

5.2 Mathematical formulation

The MILP formulation of the energetic problem is explained in the following section and it takes inspiration by the work of Wallerant [35].
The problem is set up as a Mixed Integer Linear Programming (MILP), which minimize a function of investment and operating costs. One of the most important parameters is the operating time (Δt_p), divided into periods (typical days) and each in 24 hours. The objective function at the eq.5.5 includes the investment cost (IC) and the operating cost (OP), which are correlated by the capex weight factor (α). The capex weight factor is the weighting factor of the multi-objective function and, since the solution is highly dependent on the choice of α, the factor is progressively modified in order to retrieve the Pareto front. In first place, the choice of a multi-objective function is due to the fact that it is interesting to

reach a trade-off between investment and operating cost.

$$min_{y_p^w, f_p^w, y^w, f^w} \sum_{p=1}^{P} (\sum_{w=1}^{W} OP_{1,p}^w \cdot y_p^w + OP_{2,p}^w \cdot f_p^w) \cdot \Delta t_p \cdot (1-\alpha) + \tau \cdot (\sum_{w=1}^{W} IC_1^w \cdot y^w + IC_2^w \cdot f^w) \cdot \alpha \quad (5.5)$$

where:
P is the number of periods
W is the set of technologies
y_p^w is a binary variable for the selection of the technology w for the period p
f_p^w is the size factor for the technology w for the period p
y^w is a binary variable for the selection of the technology w
f^w is the size factor for the technology w
OP is the operating cost, with 1 and 2 as fixed and variable costs
IC is the investment cost, with 1 and 2 as fixed and variable costs
τ is the cost annualization factor
α is the *capex weight factor*

The heat cascade equation (eq.5.6) ensures the heat transfer from a higher temperature interval to a lower interval, in order to close the energy balance in each set of temperatures. This concept relies on the residual heat ($R_{p,j}$), since it release the excess of heat from a higher temperature interval j to a lower interval j-1.

$$\sum_{w=1}^{W} f_p^w \cdot Q_{p,j}^w + \sum_{s=1}^{S} Q_{p,j}^s + R_{p,j+1} - R_{p,j} = 0 \quad \forall \quad p \in P, \quad j \in J \quad (5.6)$$

where:
J is the set of temperatures of the model
S is the set of process streams
P is the period of time
$Q_{p,j}^w$ is the heat release in the process
$Q_{p,j}^s$ is the heat demand in the process
$R_{p,j}$ is the residual heat

Moreover, it is necessary to constrain the residual heat at the initial and last time step within every period (eq.5.7). These time steps must both be zero, since lower and upper temperature ranges do not exist.

$$R_{p,1} = 0, \quad R_{p,N_j+1} = 0 \quad \forall \quad i = 1, 2, ..., N_j + 1, \quad p \in P \quad (5.7)$$

5.3 Technologies scenarios

The urban energy demands must match the best suited set of energy conversion technologies. In this specific work all the different technologies are chosen in order to integrate the 5G district network and targeting the self-sustainment of the neighborhood by implementing different types of long-term energy storage. Two different scenarios are presented for taking fully advantage of the DN.

5.3.1 First scenario

The first scenario is introduced to present the basic concept of the model with a CO_2 based network. The district is divided in two sections, one connected to the DN and the other using disconnected technologies, which means not taking advantage of the network as a heat source or sink. The decentralized technologies for the supply energy services, from the network to the buildings, are: heat pumps for space heating and domestic hot water, heat exchange for air cooling and CO_2 vapor compression chillers for providing the refrigeration requirement. The operating fluids are CO_2 for domestic hot water and refrigeration cycle, instead for space heating is adopted R1234yf. The buildings of the district disconnected from the network are served with heat pumps and vapor compression chillers matched with the geothermal as thermal energy source or sink.
The network for keep working requires a technology for the production of the CO_2 in the two phases (liquid and vapour), by harvesting heat from the natural sources available. This is fulfilled by the central plant (CP) and an auxiliary electric boiler for the conversion of CO_2 from liquid to vapour. The auxiliary system is integrated for avoiding an oversizing of the CP. The CP relies on the CO_2 as a working fluid, with an open cycle configuration. The CP, during the summer mode, is composed just by a condenser, so when it is required CO_2 in the liquid phase. While, along the winter mode, the CP works as a proper heat pump. Other intermediate fluids, e.g. NH_3 and $R1234yf$, should be evaluated for avoiding the high de-superheating of the cycle due to a flat saturation dome of CO_2 and considering that the high losses of the expansion valve lead to a low exergy efficiency [10]. But this evaluation, about additional refrigerants, goes beyond the scope of this work.
The electricity requirement is guaranteed by the connection to the national grid, which allows both buying and selling and the photo-voltaic panels. Furthermore a battery set enables to avoid an increasing of the costs of the market and shortage of solar irradiation.
Other technologies implemented are SOFC-GT, SOEC combined with a storage of CH_4 and the storage of CO_2 in both phases, which has been modelled according to [36]. The first scenario is represented in Fig.5.6.

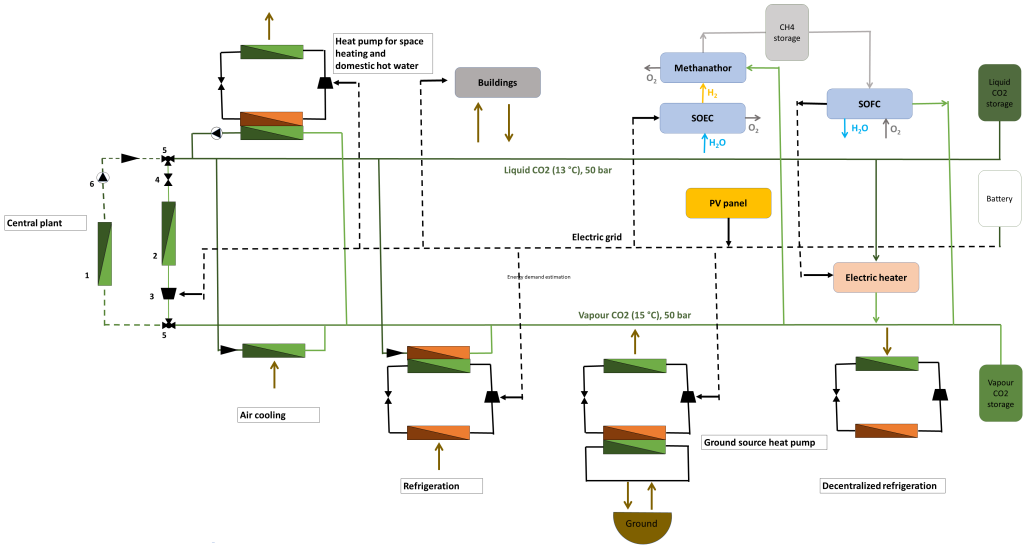

Figure 5.6: Scenario 1

5.3.2 Second scenario

The second scenario keeps same technologies as the first, but since the upside of the 5G district network is the recovery of waste heat, it is integrated a data center with its proper refrigeration system. The servers are cooled down by a system of air cooling with respectively an inlet and outlet temperature of 25°C and 40°C. The refrigerating cycle is using R410a as operating fluid to dissipate the heat generated, since is proven to be the most appropriate [37], while the ERF is equal to 0.37, using as heat sink the DN, for dissipating a DC with a power of 450kW. Hence an important amount of heat is made available to the network, with a great advantage during the winter mode, while it could cause an oversizing of the technologies along the summer mode, so it is has been evaluated the possibility of a disconnected technology for the data center. Furthermore a literature review of the traditional technologies is developed in the following section, in order to investigate the most suitable solution for the data center. The second configuration is at the Fig.5.7.

5.4 Data center heat recovery

The data centers (DCs) are facing two different problems, the growing construction being between 10-20% per year and the increasing of the power density of the microprocessors (CPUs) in the servers, which will have heat fluxes around 100 W/cm^2, while the air-cooling, the most diffused technology adopted in data centers has a maximum heat removal capacity of about 37 W/cm^2 [38], so it will not be able to handle loads in new data center design. Therefore the thermal management system is shifting from traditional air cooling to liquid or two-phase cooling [1].

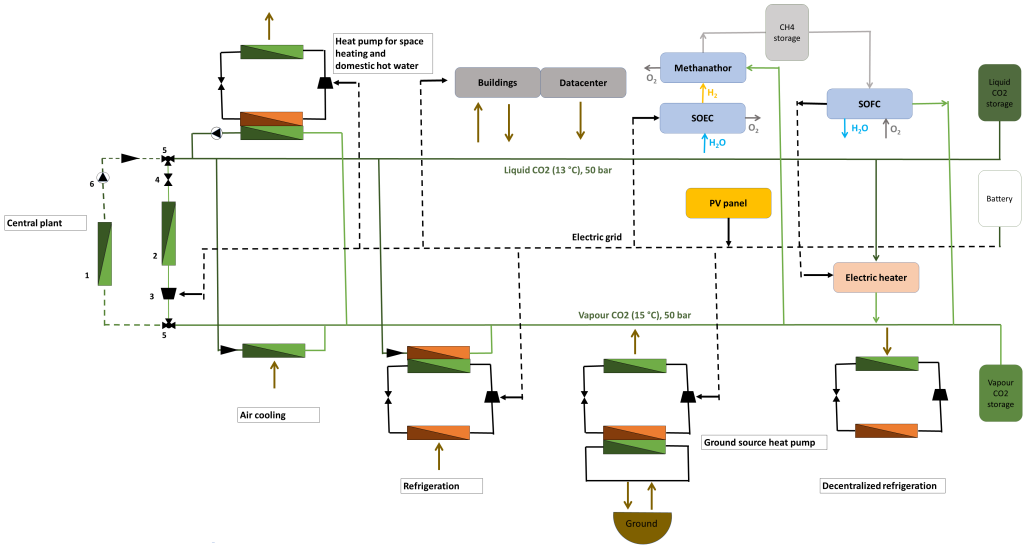

Figure 5.7: Scenario 2

Almost all the electrical power supplied to the server is dissipated into heat, necessitating the use of large scale cooling systems to keep the server in a safe operational range. This increased heat dissipation demand, increases the costs associated with powering and cooling data center [1]. The growing use of liquid cooling allows waste heat recovery to become a promising option for data center, since liquid cooling allows higher coolant temperatures than air because of its superior heat transfer [39]. This growing popularity means that liquid cooling is starting to become a more mainstream application and is no longer a niche for applications such as high-performance computing. Liquid cooling traditionally use water as cooling medium due to its ease of availability, usage and favorable thermal properties such as high heat capacity [39]. More than ever, high heat flux dissipation has become the bottleneck toward compact higher performance electronic systems [40].

5.4.1 Energy parameters of a data center

It now interesting to go through the parameters necessary to integrate a DC into an energetic model. The heat removed by a refrigeration system of a data center is evaluated with the eq. 5.8.

$$\dot{Q} = \dot{m} \cdot c_p \cdot (T_{out} - T_{in}) \tag{5.8}$$

Where $\dot{m}$ is the mass flow rate, c_p the specific heat of the fluid and the temperatures T are of inlet and outlet. The energy efficiency for data center is assumed using the power usage effectiveness (PUE); an

industry average air cooled data center has a PUE around 2,5 [41]:

$$PUE = \frac{P_{DataCenter} + P_{Cooling}}{P_{IT}}, \quad 1 \leq PUE \leq \infty \tag{5.9}$$

The PUE measures how efficiently a data center is using the electical power, and $P_{DataCenter}$ is its total consumption, $P_{Cooling}$ is the power required from the cooling system and then P_{IT} for the equipment for example regarding computing, storage and network equipment. For having good results the PUE must be as low as possible, so it implies that the data are used for computation [41]. But this parameter doesn't take into account the possibilities of a heat reuse, so has been defined also the energy reuse effectiveness ERE [41].

$$ERE = \frac{P_{DataCenter} + P_{Cooling} - P_{Reuse}}{P_{IT}} \tag{5.10}$$

And it is also evaluated the Energy Reuse Factor (ERF):

$$ERF = \frac{Reused\ energy}{Total\ Energy}, \quad 0 \leq ERF \leq 1 \tag{5.11}$$

5.4.2 Operating conditions of a data center

The heat production of a data center is relatively stable, whereas the heating load changes periodically according to the outdoor temperature, which impairs coordination between heat production and heating load [42]. The operating conditions of a data center could be summed up in:

- Full load: the system working at full computational capacity.
- Idle: the system powered on and operating without any additional computational load.

The majority of servers operate at or below 20% of their maximum power [1]

5.5 State of art cooling technologies about data centers

5.5.1 Air cooling

The air conditioning system in a legacy data center is designed based on the racks maximum power dissipation and a typical temperature rise of 15°C for the air flow. The cold air is typically supplied at 25 °C and the exhaust air leaves the room and return to the air conditioning at 40°C [1]. To solve the problem of the low quality of the heat coming from an air cooled data center it is evaluated the possibility of using an air driven heat pump, and in the [37] are studied different fluids, which with the increasing of the return air temperature, the heating capacity of the air source heat pump increases for all refrigerants.

In fact, when the temperature of the return air increases, the heat transfer rate between refrigerant and air in evaporator increases. In the study of Deymi et al. is proved that R410a has the highest heating capacity compared to other refrigerants. The COP of the air source heat pump increases for all working refrigerants when the temperature of return air increases. It can also be concluded that R134a has the best COP respect to other refrigerants so that its COP improves from 3.95 to 5.45 with increasing the return air temperature from 298 K to 303 K [37]. Similarly, the electric consumption of the air source heat pump compressor increases by increasing the return air flow rate coming from data center. It can be seen that R134a and R410a have the lowest and highest power consumption, respectively. The effect of return air temperature change from 298 K to 303 K on PUE, ERF and ERE indices of the data center using the proposed system is demonstrated in fig. **??** for R134a. Based on the obtained results, due to decreasing the mechanical cooling of the data canter using air source heat pump recovery system, PUE decreases slightly with increasing the temperature of the return air. On the other hand, increasing the return air temperature will increase reusing the waste heat of data center or heat transfer rate between refrigerant and air in evaporator and as a result ERF increases which consequently ERE decreases.

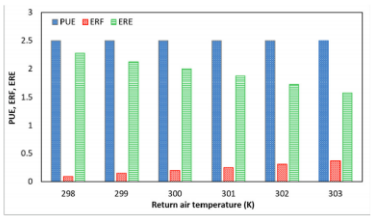

Figure 5.8: PUE,ERF and ERE ASHP R134a [1]

5.5.2 Liquid cooling

Many newer data center designs have power loadings to levels that are difficult to remove with air conditioning alone. Using a liquid cooling system we could have an input temperature of 60°C, and this allowed to keep the microprocessor temperature below 85°C, which is the technology limit for nowadays data center. This higher temperature for liquid cooling systems will provide a higher quality waste heat and the energy capture is also easier, using the direct discharge liquid stream. The heat removal capacities of more than 200 W/cm^2 [1].

5.5.3 Waste heat recovery technologies

Direct buildings heating

The temperature range of the captured waste heat from air cooled servers is more than sufficient for reuse in heating needs. It has been proposed also the possibility on installing more smaller data center

and providing heat in a decentralized way. The heat dissipated by data centers can also be used in pre-heating domestic hot water [1].
A computer server is a metal box that converts electricity into heat so has also being proposed to replace electric resistive heating elements with silicon heating elements, thereby reducing societal energy footprint by using electricity for heating to also perform computation [43]. They are integrated into the home heating system the same way as a conventional electrical furnace, using the same power system and circulation fan . This idea increase the power usage efficiencies (PUE) over conventional data centers. The disadvantages of this technology are the higher cost of electricity in residential areas and maintenance cost could increase [43].

Heat pump

The refrigeration of a data center brings the designer to deal with a safety index for the critical heat flux (CHF). This coefficient is a fundamental difference between a refrigeration system for high heat removal and for temperature regulation [44].
Among the factors to take into consideration there is the temperature of the rejected heat of the heat pump of the data center which is constant in this case, since the network glad to the central plant is keeping the values constants during time. For this work is more interesting to study the performance of the refrigeration varying the heat load to absoarb, since higher system COPs are achieved for higher heat loads, implying that the present refrigeration system is more efficient in high heat flux removal [40].
From a multi-objective point of view must be taken into account the correlation between the critical heat flux and COP since increasing the COP we decrease the critical heat flux. But we must acknowledge that all the correlation for defining the critical heat flux are defined for certain conditions, so a safety margin must be taken into account. Overcoming the critical value could lead to unfixable damages [40]. A different solution to move away from the implementation on a DN is a energy system based on a ground source heat pump (GSHP), keeping the CO_2 as operating fluid. The aim is to storage the utilization of data center waste heat during non-heating periods. Therefore, the use of soil as an energy storage container to regulate seasonal fluctuation in heating capacity is feasible. Different operation modes can be realized by applying different valve switching modes. The system can meet the cooling demands of the DC and recover waste heat for the purpose of building heating 5.9 [42].

- Free cooling: when the outdoor temperature is lower than the initial operating temperature T_i°C, CO_2 exchanges heat with outdoor air, achieving free cooling (T_i is at least 5°C below the working medium temperature).
- Direct-expansion cooling: when the outdoor temperature exceeds T_i°C, the soil works as a cold source, and gaseous CO2 discharged from the evaporator is compressed to 63.59 °C and 9 MPa. Gaseous CO_2 is cooled by transferring heat to the DHN. CO_2 is then decompressed through the expansion valve and transferred to the liquid line.

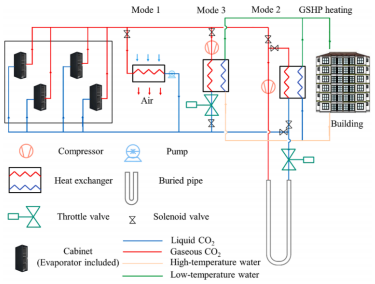

Figure 5.9: GSHP data center

- Data center as a heating source: To recover the waste heat during the heating period, CO_2 from the data center is compressed to raise its temperature, whereupon it exchanges heat with water that is used to heat the surrounding buildings.
- Ground source heat pump: during the heating period, heat stored in the soil is used to heat the surrounding building [42].

The system prioritizes the cooling of the DC and the heating of surrounding buildings, and coordinates the heating relationship by adjusting the heating power of the GSHP. Therefore, the following conditions should be met to ensure an efficient system:

1. The GSHP should be able to meet the maximum heating load. During the heating period, the heating load fluctuates. To ensure normal heating for surrounding buildings, the heating capacity of the GSHP should guarantee the building heating even when DC heating is lacking.
2. To maintain the soil temperature as constant, the heat absorbed and released by the soil should be approximately the same. Therefore, the total heat obtained from the soil during the heating period should be approximately the same as the heat stored in the soil during the non-heating period [42].

Absortion cooling

In a standard vapour compression refrigeration cycle a considerable amount of power is consumed by the compressor, in which a liquid solution of absorbent fluid and refrigerant is used, can result in considerable power savings. A typical absorption cycle, replaces the compressor with an absorbent and a generator in absorption cycle.
A typical process begins from with low pressure vapor refrigerant enters an absorber with an exothermic process where the absorbent, in a liquide state, is combined with the injected vapour. Then, the liquid solution of refrigerant and absorbent getting out the absorber is compressed to a higher pressure and gets into the solution heat exchanger, the consequent energy consumed is quite low since the difference

of pressure is rather small. The solution after going through an heat exchanger enters the generator where with an endothermic process, the refrigerant is separated from the absorbent. The exiting refrigerant vapor continues on to the condenser while the now weak liquid solution in the generator passes through an expansion valve and returns to the absorber [1].
The advantage of the the application of absorption cooling relies on not only reducing the energy necessary to run the system, but also has the benefit of using the data center waste heat as the absorption generator heat source. This technology can operate among a temperature of 70-90°C of waste heat, so it is suitable for water cooled and two phase data centers, and not for air cooled, which is an important limitation for nowadays data center [1].

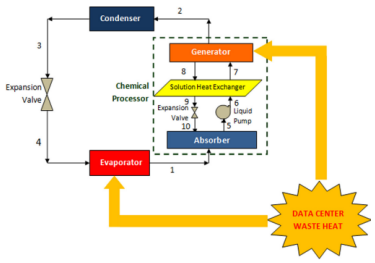

Figure 5.10: Absortion cooling system [1]

Organic Rankine Cycle

Recovering waste heat from data centers can be used to directly produce electricity through an organic Rankine cycle (ORC). Basically an ORC work following the same principle as the Rankine cycle, but using organic fluids characterized by a lower boiling points. The lower boiling points make it possible for data center waste heat to serve as heat source. Common organic fluids include R-134a, Benzene, Toluene and Propane with operating temperature ranges as wide as 65–350 °C [1], which could be an interesting technology for for a water or two-phase cooled data center. Despite a low overall efficiency, between 5% and 20 %, due to a low operating temperature, which brings also an air cooled data center to be suitable if combined with an additional heat source. This technology is useful in the context of this work if it is not convenient to approach an heat recovery of the data center, due to an oversizing of the central plant driving the model model to a not economical sustainability [1].

5.6 Results and discussion

In order to evaluate the results is important to underline the peaks of demands related to the typical days, since they size the integrated technologies of each scenario.
The power peaks are 12.4 MW and 7.1 MW respectively for heating and cooling demand. Among the

heat demand, the 12.1% is for domestic hot water and 87.9% is for space heating, while in correspondence of the cooling peak, the 2.8% is attributed to air cooling and 97.2% to the refrigeration.

5.6.1 Results first scenario

About the first scenario, a economical analysis is performed keeping into consideration the two parameters adopted for the results generation; the *network factor* and the *capex weight factor*. The *network factor* defines the fraction of buildings connected to the network, while *capex weight factor* (CWF) is the weighting factor (α) of the objective function for the energetic model(eq.5.5). By the variation of the two parameters just described is generated a Pareto plot as in fig. 5.11, where is assumed to avoid any constrain to the electric grid. To generate the plot is assumed a *capex weight factor* between 0 and 1, and it can be be verified how at the decreasing of the *network factor* both investment and operating costs are increasing, due to the more expensive decentralized technologies and lack of the network as a thermal source. In order to generate the Pareto front are used low *capex weight factors*, since the investment cost is way larger than the operating cost, thus the changes of the sizing are more important at low *capex weight factors*.

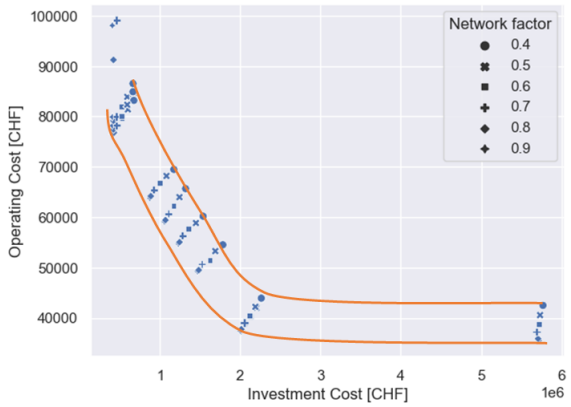

Figure 5.11: Pareto with no grid limitations

An analysis about the first scenario is based on a constant *capex weight factor* (CWF) and retrieving the investment cost of the technologies. For the fig. 5.12 the factor CWF is equal to 0.01. Since the CWF is low the PV panels are always chosen for a cost of 1.584 kCHF, so it isn't plotted in figure for graphic reasons. At the increasing of the *network factor* the not connected technologies are decreasing in size and the opposite trend for the network based technologies. Another constantly chosen technology is the electric heater which is useful to limit the maximum size of the central plant, in order to avoid an oversizing. The same advantage is got by the increasing of the CO_2 tanks, both liquid and vapour, which is actually obtained at the expansion of the network through the district.
The *blu point* in the fig. 5.12 defines the investment cost of the network, referred to the correspondent

network factor (NF). The model reaches a minimum at a NF of 0.8, where the 79.2% of the costs are covered by PV panels, which is clearly the most important investment. The decentralize technology are respectively 0.09% and 0.07% for the ones connected to the DN and the standalone. The rest is taken by central plant, CO_2 tanks and electric heaters.

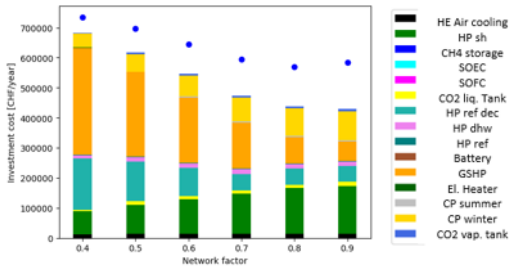

Figure 5.12: Constant capex weight factor for the first scenario

Another approach is represented in fig. 5.13, where for a constant *network factor*, equal to 0.8, is imposed the *capex weight factor* as a discrete variable and by running the model are retrieved the investment costs; since it is undoubtedly the most convenient configuration of the network. At the increasing of CWF the tanks and PV panels are lower and lower, as the electric heater. The PV panels have the biggest variation, moving from 79.2% with the lowest CWP to 42.7% when CWP is equal to 0.026, the same trend for CO_2 tanks but way less important on the total, from 0.76% to 0.36%.

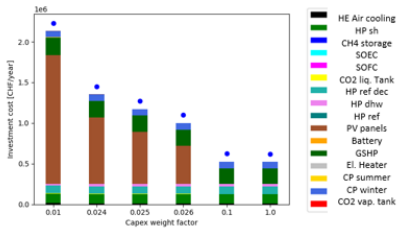

Figure 5.13: Constant network factor for the first scenario

The superstructure includes also a battery and power-to-gas units, not chosen since the model found cheaper to oversize the electric grid. The electric grid is characterized by an operating cost of either import or export, as it is pointed out in the appendix A. So another consideration is to limit the maximum power of the electric grid, which brings to the generation of a new Pareto graph in fig. 5.14. The maximum size of the electric grid is imposed by imposing the higher amount of energy imported or exported in one time step.

In this configuration the system select the power-to-gas for filling the lack of electrical power of the system and for a *CWF* of 0.01 is interesting how the model reacts, since with a small DN is necessary an

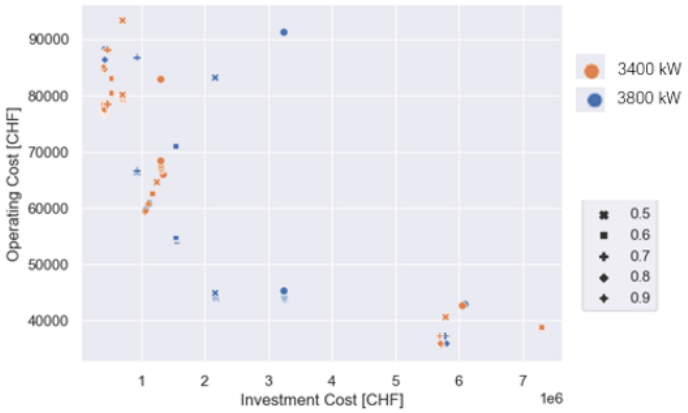

Figure 5.14: Pareto with electric grid limitation

high size of storages. The maximum size of the the whole power-to-gas 0.02%, due to a selling price of the electricity always lower than the buying price, and the CH_4 grid is not connected to the global one, so the fuel cell consumes all the produced CH_4. While the PV panels are taking from 49% to 0% at the increasing of the network, due to the decreasing of energy consumption, glad to the a more and more usage of the DN as heat and sink source.

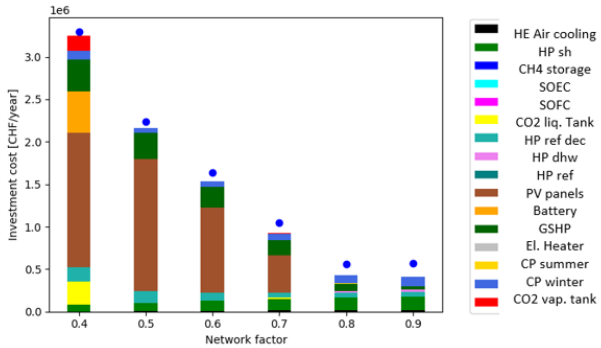

Figure 5.15: Constant network factor with grid limitation for the first scenario

5.6.2 Results second scenario

In this section is performed the results analysis of the second scenario. By the combination of the *capex weight factor* and the *network factor* is retrieved the Pareto plot in fig. 5.16, where both investment and operating cost are higher, due to the electric consumption and the refrigeration required to dissipate the heat generated by the data center. This behaviour was expected and to fully take advantage of the data

center integration must be set a constrain to the electric grid, as it is performed in the following part of this section.

Figure 5.16: Pareto with DC integration

A set of configurations is proposed by keeping as constant the *capex weight factor* and as a discrete variable the *network factor*. For the Fig. 5.17 the factor CWF is imposed to 0.01, since it is the most promising value, since its set of solution is the closest to the utopia point [45]. Furthermore, the connection to the data center occurs just in correspondence of 0.7 of the total network, hence are plotted just three cases, where the PV panels (1.584.616 CHF) have the maximum available size, but the value isn't plotted due to a graphic reason. Comparing the second scenario with the first at the Fig. 5.12, it results in a saving on the size of CO_2 tanks and central plant in the winter mode, but it's completely balanced by the central plant from the summer mode, so from the investment cost point of view the refrigeration of the data center is zero-cost.

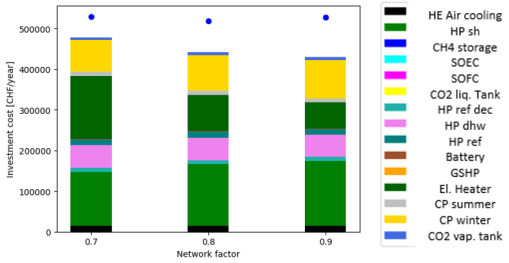

Figure 5.17: Constant network factor for the second scenario

The previous discussion assumes to connect the data center to the network for a waste heat recovery, but it could nevertheless taken into consideration the configuration of not connected technology, since not evaluating different options could lead to a misleading optimization. The comparing of the two cases results in a difference of investment and operating cost, hence in the fig. 5.18 is quantified the upside of connecting the data center to the DN. The savings in this case scenario is around 42.000 CHF per year in terms of operating costs, which is pretty consistent considering it covers around 51% of the minimum

operating cost of a data center not connected to the DN.

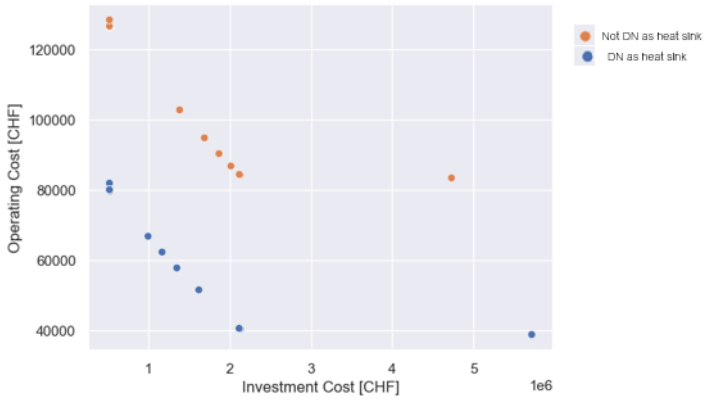

Figure 5.18: Connection of the data center

6
Conclusion

The rapid climate change requires a highly integrated system to achieve the next goals in terms of a reduction of the energy consumption and to overcome the technological limitations of the renewable energy; intermittence and fluctuation of energy production. The 5G district network has been pointed as the proper way to approach this challenge, in particular a network based on CO_2 as the working fluid.
The method presented integrates a superstructure of technologies for energy conversion, with an algorithm for the construction of a district network in a chosen neighborhood, by taking advantage of the available streets. The proposed method adopts a double optimization approach, in order to facilitate the analysis and looping the two processes to achieve the different configurations of the network, that rely on the progressive coverage ratio of the network through the neighborhood. In this work it has been analyzed the district of Ronquoz in Sion (Switzerland), in order to prove the reliability of the method. This neighborhood, after a requalification, is going to have 192 buildings mixed with 37% of residential, 55% of general activities and 8% of commercial. In order to estimate the energy demand for each service and building, it has been adopted the energy signature model, which is based on a linear regression.
The first optimization loop comes after retrieving the energy requirements. Here it is possible, thanks to a system of equations, to build the district network as a tree graph by minimizing the investment cost of the pipes. The objective function is dependent on the length and the section of the pipes and since the solver is linear and the function of the investment cost is non-linear, in the post-processing, it is developed a refinement of the results. The operating costs are assumed as the electricity bill of winning the pressure losses along the network, since a change of phase of the CO_2 could drive the system to not working properly. Hence, some boosters are spread all over the network and the cost taken into consideration is just about the electrical consumption. A set of network configurations are generated with a loop over the power provided by the central plant, in order to accomplish a progressive coverage of the

neighborhood.
After the network's branch, the method moves to the development of the energetic model, which is the second optimization loop. Firstly the model is kept without any electric grid constrains, thus the selected technologies are all the decentralized HPs, the central plant, the electric heater and in small part the CO_2 tanks. A more integrated and standalone system is achieved by limiting the maximum power of the electric grid, when also power-to-gas, batteries and CH_4 cover an important role for the minimization of the costs. Moreover, a different superstructure of technologies, with the connection of the data center to the district network, brings an increasing of about 40 kCHF in operating cost in the best case scenario, while the investment costs are balanced to the reduction of the size of the central plant in the winter mode.
By merging the results, in the specific case of Ronquoz, a minimum is found with the connection of the 80% of the buildings to the network, by optimizing for the starting point which is one of the most sensible parameter since the spatial position of the buildings, with their demand, is thoroughly analysed.
The future work includes the analysis of the self-sufficiency of the neighborhood, by running the model with a whole year of weather forecast and adopting a more powerful device for the computation of the model. Another interesting aspect could be studying the district from a macro prospective, by implementing an CH_4 grid if the other suburbs in the city requires it and integrating new technologies to the superstructure (e.g. hydroelectric), which could reduce the costs of the other storages.
The data center will face new refrigeration development e.g. the liquid cooling system of the racks, for achieving a higher specific power of the units, so also the technology for the heat recovery could improve, thus the model can integrate a data center with a CO_2 refrigeration system in order to achieve a more integrated district network.

References

[1] K. Ebrahimi, G. F. Jones, and A. S. Fleischer, "A review of data center cooling technology, operating conditions and the corresponding low-grade waste heat recovery opportunities," *Renewable and Sustainable Energy Reviews*, vol. 31, pp. 622–638, 2014.

[2] worldbank. worldbank: urban development. [Online]. Available: https://data.worldbank.org/topic/urban-development

[3] J. O. Lewis, S. Ní Hógáin, and A. Borghi, "Cities of tomorrow–action today. urbact ii capitalisation. building energy efficiency in european cities," 2013.

[4] P. Stadler, L. Girardin, A. Ashouri, and F. Maréchal, "Contribution of model predictive control in the integration of renewable energy sources within the built environment," *Frontiers in Energy Research*, vol. 6, p. 22, 2018.

[5] I. Sartori, A. Napolitano, and K. Voss, "Net zero energy buildings: A consistent definition framework," *Energy and buildings*, vol. 48, pp. 220–232, 2012.

[6] D. Baker and S. Sherif, "Heat transfer optimization of a district heating system using search methods," *International Journal of Energy Research*, vol. 21, no. 3, pp. 233–252, 1997.

[7] H. Lund, S. Werner, R. Wiltshire, S. Svendsen, J. E. Thorsen, F. Hvelplund, and B. V. Mathiesen, "4th generation district heating (4gdh): Integrating smart thermal grids into future sustainable energy systems," *Energy*, vol. 68, pp. 1–11, 2014.

[8] S. Henchoz, P. Chatelan, F. Maréchal, and D. Favrat, "Key energy and technological aspects of three innovative concepts of district energy networks," *Energy*, vol. 117, pp. 465–477, 2016.

[9] G. Lorentzen, "Revival of carbon dioxide as a refrigerant," *International journal of refrigeration*, vol. 17, no. 5, pp. 292–301, 1994.

[10] S. Henchoz, C. Weber, F. Maréchal, and D. Favrat, "Performance and profitability perspectives of a co2 based district energy network in geneva's city centre," *Energy*, vol. 85, pp. 221–235, 2015.

[11] J. E. Anderson, G. Wulfhorst, and W. Lang, "Energy analysis of the built environment—a review and outlook," *Renewable and Sustainable Energy Reviews*, vol. 44, pp. 149–158, 2015.

[12] R. Lund and S. Mohammadi, "Choice of insulation standard for pipe networks in 4th generation district heating systems," *Applied Thermal Engineering*, vol. 98, pp. 256–264, 2016.

[13] T. Falke, S. Krengel, A.-K. Meinerzhagen, and A. Schnettler, "Multi-objective optimization and simulation model for the design of distributed energy systems," *Applied Energy*, vol. 184, pp. 1508–1516, 2016.

[14] B. Morvaj, R. Evins, and J. Carmeliet, "Optimising urban energy systems: Simultaneous system sizing, operation and district heating network layout," *Energy*, vol. 116, pp. 619–636, 2016.

[15] J. von Rhein, G. P. Henze, N. Long, and Y. Fu, "Development of a topology analysis tool for fifth-generation district heating and cooling networks," *Energy conversion and management*, vol. 196, pp. 705–716, 2019.

[16] L. Girardin, F. Marechal, M. Dubuis, N. Calame-Darbellay, and D. Favrat, "Energis: A geographical information based system for the evaluation of integrated energy conversion systems in urban areas," *Energy*, vol. 35, no. 2, pp. 830–840, 2010.

[17] B. Dong, S. E. Lee, and M. H. Sapar, "A holistic utility bill analysis method for baselining whole commercial building energy consumption in singapore," *Energy and buildings*, vol. 37, no. 2, pp. 167–174, 2005.

[18] M. Bauer and J.-L. Scartezzini, "A simplified correlation method accounting for heating and cooling loads in energy-efficient buildings," *Energy and Buildings*, vol. 27, no. 2, pp. 147–154, 1998.

[19] R.-A. Suciu, "Fifth generation district energy systems for low carbon cities," EPFL, Tech. Rep., 2019.

[20] L. Girardin, "A gis-based methodology for the evaluation of integrated energy systems in urban area," EPFL, Tech. Rep., 2012.

[21] Ronquoz21. Ronquoz21 plan. [Online]. Available: https://www.sion.ch/_docn/2388641/test.pdf

[22] B. Talebi, P. A. Mirzaei, A. Bastani, and F. Haghighat, "A review of district heating systems: modeling and optimization," *Frontiers in Built Environment*, vol. 2, p. 22, 2016.

[23] L. T. Biegler and I. E. Grossmann, "Retrospective on optimization," *Computers & Chemical Engineering*, vol. 28, no. 8, pp. 1169–1192, 2004.

[24] D. Dobersek and D. Goricanec, "Optimisation of tree path pipe network with nonlinear optimisation method," *Applied thermal engineering*, vol. 29, no. 8-9, pp. 1584–1591, 2009.

[25] C. Bordin, A. Gordini, and D. Vigo, "An optimization approach for district heating strategic network design," *European Journal of Operational Research*, vol. 252, no. 1, pp. 296–307, 2016.

[26] J. Söderman and F. Pettersson, "Structural and operational optimisation of distributed energy systems," *Applied thermal engineering*, vol. 26, no. 13, pp. 1400–1408, 2006.

[27] J. Söderman and P. Ahtila, "Optimisation model for integration of cooling and heating systems in large industrial plants," *Applied Thermal Engineering*, vol. 30, no. 1, pp. 15–22, 2010.

[28] C. Haikarainen, F. Pettersson, and H. Saxén, "A model for structural and operational optimization of distributed energy systems," *Applied Thermal Engineering*, vol. 70, no. 1, pp. 211–218, 2014.

[29] I. Baldvinsson and T. Nakata, "Cost assessment of a district heating system in northern japan using a geographic information–based mixed integer linear programming model," *Journal of Energy Engineering*, vol. 143, no. 3, p. F4016006, 2017.

[30] C. Weber and D. Favrat, "Conventional and advanced co2 based district energy systems," *Energy*, vol. 35, no. 12, pp. 5070–5081, 2010.

[31] S. P. Peletiri, N. Rahmanian, and I. M. Mujtaba, "Co2 pipeline design: A review," *Energies*, vol. 11, no. 9, p. 2184, 2018.

[32] G. O. Brown, "The history of the darcy-weisbach equation for pipe flow resistance," in *Environmental and water resources history*, 2003, pp. 34–43.

[33] N. Azizi, R. Homayoon, and M. R. Hojjati, "Predicting the colebrook–white friction factor in the pipe flow by new explicit correlations," *Journal of Fluids Engineering*, vol. 141, no. 5, 2019.

[34] N. Kaoungku, K. Suksut, R. Chanklan, K. Kerdprasop, and N. Kerdprasop, "The silhouette width criterion for clustering and association mining to select image features," *International journal of machine learning and computing*, vol. 8, no. 1, pp. 1–5, 2018.

[35] A. S. Wallerand, M. Kermani, R. Voillat, I. Kantor, and F. Maréchal, "Optimal design of solar-assisted industrial processes considering heat pumping: Case study of a dairy," *Renewable Energy*, vol. 128, pp. 565–585, 2018.

[36] E. Facchinetti, D. Favrat, and F. Marechal, "Innovative hybrid cycle solid oxide fuel cell-inverted gas turbine with co2 separation," *Fuel Cells*, vol. 11, no. 4, pp. 565–572, 2011.

[37] M. Deymi-Dashtebayaz and S. Valipour-Namanlo, "Thermoeconomic and environmental feasibility of waste heat recovery of a data center using air source heat pump," *Journal of Cleaner Production*, vol. 219, pp. 117–126, 2019.

[38] D. Wu, "Experimental evaluation and control of two-phase multi-microchannel evaporator cooling systems for high efficiency data center," EPFL, Tech. Rep., 2012.

[39] R. Khalid, S. Schon, A. Ortega, and A. Wemhoff, "Waste heat recovery using coupled 2-phase cooling & heat-pump driven absorption refrigeration," in *2019 18th IEEE Intersociety Conference on Thermal and Thermomechanical Phenomena in Electronic Systems (ITherm)*. IEEE, 2019, pp. 684–692.

[40] R. Zhou, T. Zhang, J. Catano, J. T. Wen, G. J. Michna, Y. Peles, and M. K. Jensen, "The steady-state modeling and optimization of a refrigeration system for high heat flux removal," *Applied Thermal Engineering*, vol. 30, no. 16, pp. 2347–2356, 2010.

[41] S. Zimmermann, I. Meijer, M. K. Tiwari, S. Paredes, B. Michel, and D. Poulikakos, "Aquasar: A hot water cooled data center with direct energy reuse," *Energy*, vol. 43, no. 1, pp. 237–245, 2012.

[42] X. Wang, H. Li, Y. Wang, J. Zhao, J. Zhu, S. Zhong, and Y. Li, "Energy, exergy, and economic analysis of a data center energy system driven by the co2 ground source heat pump: Prosumer perspective," *Energy Conversion and Management*, vol. 232, p. 113877, 2021.

[43] J. Liu, M. Goraczko, S. James, C. Belady, J. Lu, and K. Whitehouse, "The data furnace: Heating up with cloud computing." in *HotCloud*, 2011.

[44] Y. Katto and H. Ohno, "An improved version of the generalized correlation of critical heat flux for the forced convective boiling in uniformly heated vertical tubes," *International journal of heat and mass transfer*, vol. 27, no. 9, pp. 1641–1648, 1984.

[45] I. Santín, C. Pedret, and R. Vilanova, *Control and decision strategies in wastewater treatment plants for operation improvement*. Springer, 2016, vol. 86.

[46] S. Henchoz, "Potential of refrigerant based district heating and cooling networks," EPFL, Tech. Rep., 2016.

[47] L. Wang, M. Pérez-Fortes, H. Madi, S. Diethelm, F. Maréchal *et al.*, "Optimal design of solid-oxide electrolyzer based power-to-methane systems: A comprehensive comparison between steam electrolysis and co-electrolysis," *Applied Energy*, vol. 211, pp. 1060–1079, 2018.

[48] R. Suciu, P. Stadler, A. Ashouri, and F. Maréchal, "Towards energy-autonomous cities using co2 networks and power to gas storage," Tech. Rep., 2016.

[49] I. Sarbu and C. Sebarchievici, "General review of ground-source heat pump systems for heating and cooling of buildings," *Energy and buildings*, vol. 70, pp. 441–454, 2014.

[50] A. M. Omer, "Ground-source heat pumps systems and applications," *Renewable and sustainable energy reviews*, vol. 12, no. 2, pp. 344–371, 2008.

[51] O. Ozgener and A. Hepbasli, "Modeling and performance evaluation of ground source (geothermal) heat pump systems," *Energy and Buildings*, vol. 39, no. 1, pp. 66–75, 2007.

A

A.1 Central plant

The central plant (CP) is required for balancing the DN, since there is a lack of CO_2 in the phase of liquid during the summer and of vapour along the winter. The excess of heat is dissipated thanks to a lake, which during the summer is still enough cold. Another advantage of the following set up of the CP is realized when the condenser exchange heat with the lake, in this condition is just necessary to pump the fluid and not compressing it, with savings in term of electricity. Instead during the winter mode the CP works as a proper heat pump, with a compressor with a non negligible amount of electricity.
The selected technology for the central plant is a CO_2 open cycle. Other intermediate fluids like NH_3 or $R1234yf$ should be evaluated for avoiding the high de-superheating of the cycle due to a flat saturation dome of CO_2 and high losses of the expansion valve, bring this configuration to have a low exergy efficiency [10]. But considering additional settings goes beyond the scope of this work.
The components of a CP are roughly just a CO_2 condenser for summer operation and an evaporator which uses heat form the lake water to evaporate the refrigerant in the heat pump. The sizing of the central plant is usually calculated in the worst conditions, since it is key part of the whole model.
The fig.A.1 shows the CP as it is implemented in the model and the components are listed in the Table A.1.

The temperature of the liquid pipes are constrained by the summer mode when it must be high enough to exchange heat with the lake and low enough to have free cooling for air conditioning, so we define a minimum (eq.A.1) and maximum (eq.A.2) temperature.

$$T_{liquid,min} = T_{lake} + \Delta T_{lake} + \Delta T_{min,rw} \tag{A.1}$$

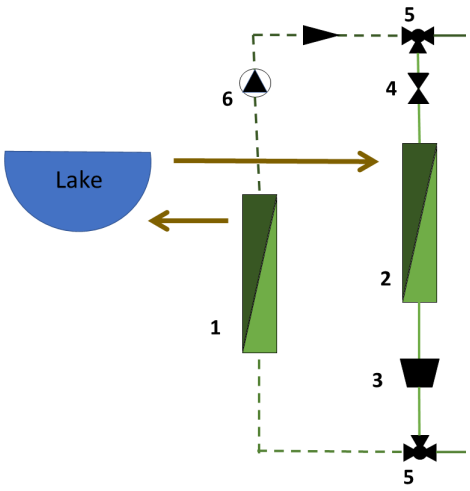

Figure A.1: Configuration central plant

1	Condenser
2	Evaporator
3	Compressor
4	Expansion Valve
5	3-way valve
6	Circulation Pump

Table A.1: Components of the central plant

$$T_{liquid,max} = T_{AC} - \Delta T_w - \Delta T_{min,rw} \tag{A.2}$$

Where T_{AC} is the temperature for air cooling, T_{lake} is the temperature of the lake, with ΔT_{lake} the minimum difference of the temperature between inlet and outlet for the water. Furthermore $\Delta T_{min,rw}$ is due to the heat exchanger.

The assumption for the costs in CHF respectively of heat exchangers, compressors are [46]:

$$Cost_{heat_exchanger} = 420 \cdot Area_{exchange} + 147 \tag{A.3}$$

$$Cost_{comp} = (154 \cdot \dot{V}^{0.84} + 224) \cdot (P_{out}/20)^{0.41} \cdot (P_{in}/682)^{0.19} \tag{A.4}$$

Where:

$Area_{exchange}$ is the exchange are in m^2

P_{out} is the pressure at the outlet in bar
P_{in} is the pressure at the inlet in
$\dot{V}^{0.84}$ is the volume flow rate in m^3/h

The following section it is a description of the parameters for the model with $Cost_{inv,1}$ and $Cost_{inv,2}$ respectively equal to 5680 CHF and 1240 CHF/kW. The heat exchager for the summer mode are hence $Cost_{inv,1}$ and $Cost_{inv,2}$ respectively equal to 184 CHF and 197 CHF/kW [19]. These values are valid also for the future units.

Units:

- Central plant winter: it converts a certain quantity of liquid CO_2 into vapour:

Unit -	F_{min} [kg/s]	F_{max} [kg/s]	Cost1 [CHF]	Cost2 [CHF/(kg/s)]	Cinv1 [CHF]	Cinv2 $[kg_{CO_2}/(kg/s)]$
CP_{winter}	0	$F_{max,cp,liq}$	0	0	Cinv1	Cinv2

Streams:

Type	Layer	In/Out of the layer	Value
$CO2_{cp,in}$	$CO2_{liq}$	In	3.6
$CO2_{cp,out}$	$CO2_{vap}$	Out	3.6
$Elec_{cp,n}$	elec	In	HP_E

- Central plant summer: it converts a certain quantity of vapour CO_2 into liquid:

Unit -	F_{min} [kg/s]	F_{max} [kg/s]	Cost1 [Euro]	Cost2 [Euro/(kg/s)]	Cinv1 [Euro]	Cinv2 [Euro/(kg/s)]
CP_{winter}	$F_{max,cp,vap}$	$F_{max,cp,vap}$	0	0	$Cinv1_{hex}$	$Cinv2_{hex}$

Streams:

Type	Layer	In/Out of the layer	Value
$CO2_{cp,in}$	$CO2_{liq}$	Out	3.6
$CO2_{cp,out}$	$CO2_{vap}$	In	3.6

A constrain equation is implemented to avoid to keep central plant as winter and summer mode in the same time step (eq. A.5).

$$Use_{CP,winter,t} + Use_{CP,summer,t} \leq 1 \tag{A.5}$$

Where $Use_{CP,winter,t}$ and $Use_{CP,summer,t}$ are binary parameters equal to 0 if the technology isn't selected and to 1 if the technology is chosen.
Other parameters are defined in order to complete the model:

- Investment cost:

$$C_{inv,1} = Cost_{inv,1} \cdot \frac{i \cdot (1+i)^n}{(1+i)^n - 1} \tag{A.6}$$

$$C_{inv,2} = Cost_{inv,2} \cdot \frac{i \cdot (1+i)^n}{(1+i)^n - 1} \cdot HP_E \tag{A.7}$$

$$C_{inv,1,hex} = Cost_{inv,1,hex} \cdot \frac{i \cdot (1+i)^n}{(1+i)^n - 1} \tag{A.8}$$

$$C_{inv,2,hex} = Cost_{inv,2,hex} \cdot \frac{i \cdot (1+i)^n}{(1+i)^n - 1} \cdot HP_{Q,cp,w} \tag{A.9}$$

- Energy:

$$HP_E = m \cdot \frac{h_{cond,inlet} - h_{evap,out}}{\eta_{mec}} \tag{A.10}$$

$$HP_Qc, w = m \cdot (h_{cond,inlet} - h_{cond,out,subcooled}) \tag{A.11}$$

- Flow rate:

$$m = \frac{h_{evap}}{h_{cond,inlet} - h_{cond,outlet,subcooled}} \tag{A.12}$$

A.2 Photovoltaic panel

The solar energy valorization is allowed by the installation of PV panels to produce electricity, harvesting solar energy. The PV are modeled as follow, with A^{PV} the PV area, η^{PV} the PV efficiency, I the irradiation of the sun, T^{PV} the PV temperature, U^{glass} the thermal transmission coefficient, T^{ext} the ambient temperature, and f^{glass} the factor which quantify the solar irradiation passing through the PV glass. In addition the reference values are set as in the Table A.2 [19].

Parameter	Value	Unit
$T^{PV,ref}$	298	K
U^{glass}	29.1	$W/(m^2 \cdot K)$
f^{glass}	0.9	-
$\eta^{PV,ref}$	0.14	-
$\eta^{PV,var}$	0.001	1/K

Table A.2: PV parameters

$$\dot{m}_{PV,electricity}(t) = A^{PV}(t) \cdot \eta^{PV}(t) \cdot I(t) \tag{A.13}$$

$$\eta^{PV}(t) = \eta^{PV,ref} - \eta^{PV,var} \cdot (T^{PV}(t) - T^{PV,ref}) \tag{A.14}$$

$$T^{PV} = \frac{U^{glass} \cdot T^{ext}(t)}{U^{glass} - \eta^{PV,ref} - \eta^{PV,var} \cdot I(t)} + \frac{I(t) \cdot (f^{glass} - \eta^{PV,ref} \cdot T^{PV,ref})}{U^{glass} - \eta^{PV,var} \cdot I(t)} \tag{A.15}$$

Since the analysis of the available roof's surface requires more topological data, it has been used the correlation based on the footprint of the buildings regarding a typical central European urban center, 0.27 m^2_{ERA}/m^2_{footpr} [19]. Since the footprint of Ronquoiz is 192.000 m^2, it is supposed of having a maximum installed surface of 51840 m^2, with an average price of 246.9 EUR/m^2 [19].
In the the energetic model the parameters are as in Table A.3.

Unit -	F_{min} [m^2]	F_{max} [m^2]	$Cost_1$ [Euro]	$Cost_2$ [Euro/(m^2)]	$Cinv_1$ [Euro]	$Cinv_2$ [Euro/(m^2)]
PV Panel	0	51840	0	0	0	246.9

Table A.3: PV parameters for the energetic model

A.3 Energy grids

A.3.1 Electricity grid

The yearly consumption of electricity is around 14347 MWh, which takes into account just the demand of the buildings. Regarding the price of the electricity is assumed a difference of price between day and night schedule in both modes; selling and buying. As in the fig.A.2 the sell price is always lower of the buy price, so it is avoided to implement an equation for constraining the use of both units at the same time step.

A.4 SOEC-SOFC

It has been considered a SOFC-gas turbine hybrid cycle where the fuel feeding the system is methane, which undergo to a steam reforming. The reformed fuel is driven to the anode of the SOFC and the outside is mixed with an oxidizer in order to realize a complete combustion before entering the gas turbine and realizing the production of electricity [36]. The solid oxide electrolyzer cell (SOEC) and methanatorare modelled according to [47]. But for this project it has been extremely simplified, avoiding to include H_2O.
In addiction the heat stream are converted in CO_2, so the SOFC absorbs vapour of CO_2 and the SOEC

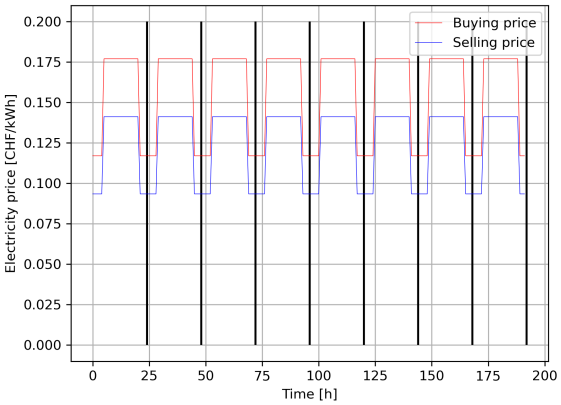

Figure A.2: Electricity grid price

is generating vapour CO_2.
These are combined with a storage of CH_4. The efficiencies are taken considering a HHV of 141.75 kJ/kg for H_2 and 43000 kJ/Kg for CH_4, as listed in the following equations:

$$\eta_{H_2} = \frac{\dot{m}_{H_2} \cdot HHV_{H_2}}{\dot{m}_{el}} = 94\% \tag{A.16}$$

$$\eta_{el} = \frac{\dot{m}_{el}}{HHV_{CH_4} \cdot \dot{m}_{CH_4}} = 75\% \tag{A.17}$$

$$\eta_{th} = \frac{\dot{Q}_{SOFC}}{HHV_{CH_4} \cdot \dot{m}_{CH_4}} = 20\% \tag{A.18}$$

A.5 Storage tanks

The generic energy balance governing the storage tank is expressed by the eq. A.19, where f refers to the device charge or discharge, depending on the sign. The losses are modelled with σ as the self-discharged rate of the unit, and $\eta_{ch} = \eta_{dch}$ as the charging and discharging efficiencies of the unit.

$$f_{u,t+1} = \sigma \cdot f_{u,t} + \eta_{ch} \cdot f^{+}_{u,t} - \frac{f^{-}_{u,t}}{\eta_{dch}} \quad \forall \quad u \in Unit, \quad t \in Timestep \tag{A.19}$$

In this work are integrated four type of storages, two for the phases of the CO_2, one for electricity and the last about $CH4$. The liquid CO_2 is stored at the operating network pressure and temperature of 5 MPa and 13 °C, while the vapour CO_2 storage is kept at MPa and 15 °C. The losses are modelled with

σ=0.9992 as the self-discharged rate of the unit, and $\eta_{ch} = \eta_{dch}$=0.95 as the charging and discharging efficiencies of the unit.
The methane is stored as a liquid, at a pressure of 1 bar and at the temperature of -162 °C for keeping the liquid state. Regarding the losses are kept the same parameters as for the CO_2 [48]. The stationary batteries are modelled using a single state dynamic model with a self-discharged rate (σ) of 1 and the charging efficiency ($\eta_{ch} = \eta_{dch}$) of 0.90. Moreover for avoiding a premature degradation of the battery, a minimum and maximum level of storage is fixed, BAT_{min} and BAT_{max} of respectively 0.2 and 0.8 [19].

$$f_{BAT,t} \geq BAT_{min} \cdot f_{BAT,max} \quad \forall \quad t \in Timestep \tag{A.20}$$

$$f_{BAT,t} \leq BAT_{max} \cdot f_{BAT,max} \quad \forall \quad t \in Timestep \tag{A.21}$$

A.6 Ground Source Heat Pump

The ground source heat pump (GSHP) is widely diffuse for heating and air conditioning, using the ground as a heat source in heating and a heat sink in cooling mode. For exchanging heat with the ground are installed a sealed loop of pipes, where usually circulates water. The depth of the borehole is within a range of 40 m and 150 m. The efficiency of the GSHP is higher than the air source heat pump since the ground has higher stability [49] about the temperature. This technology has been preferred to the gasboiler, since there is no "blast" of hot air, so it provides a constant heat [50].

A.6.1 Model of the GSHP

The COP takes into account the work of the pumps for water circulation:

$$COP_{sys} = \frac{\dot{Q}_{cond}}{\dot{W}_{comp} + \dot{W}_{pumps}} \tag{A.22}$$

The mode is caracterized by using water injected through vertical pipes, exchanging with the heat pump thanks to an heat exchanger [51].
In a steady state model the heat exchanged with the ground is:

$$\dot{Q}_{ground} = \dot{m}_w \cdot C_{p,w} \cdot (T_{out,w} - T_{in,w}) \tag{A.23}$$

where:
Q_{ground} is the heat to transfer in kW
m_w is the mass flow rate of the boreholes in kg/s

$C_{p,w}$ is the specific heat of the water in (kJ/kg K)
$T_{out,w}$-$T_{in,w}$ are the temperatures of outlet and inlet in K

$$L = \frac{Q_{ground} \cdot R_g}{t_g - t_f} \tag{A.24}$$

where:
t_g is the temperature of the ground in K,
t_f is the temperature of the working fluid in K,
R_g is the effective thermal resistance of ground per unit of length mK/kW,

The parameters for the modelling the GSHP require the cost of the boreholes per meter and the dissipation quantities of heat [49].

R_b	[(mK)/W]	0.09
Length boreholes	[m]	1500
Cost boreholes	[CHF]	44544
Cost boreholes per meter	[CHF/m]	29.69

Table A.4: Parameters of GSHP

A.7 Heat pumps

The parameter that characterize the heat pump is the coefficient of performance (COP) and it depends on the temperature demand of the different services and to the minimum difference temperature of the heat exchangers. This temperature is up the design of the heat exchanger and are set, with various combination, to $\Delta T_{water-water}$ =4 °C, $\Delta T_{water-refr}$ =1.5 °C and $\Delta T_{refr-refr}$ =1 °C.
The COPs for surface heating, district heating water and for refrigeration are respectively the eq. A.25 and A.26 [48].

$$COP_{SH,DHW} = \frac{T_{cond}}{T_{cond} - T_{evap}} \cdot \eta_{carnot} \tag{A.25}$$

$$COP_{REF} = \frac{T_{evap}}{T_{cond} - T_{evap}} \cdot \eta_{carnot} \tag{A.26}$$

with:

$$\eta_{carnot} = \eta_{el,mot} \cdot \eta_{transm} \cdot \eta_k \tag{A.27}$$

where:
$\eta_{el,mot}$ is the efficiency of the electric motor
η_{transm} is the efficiency of the transmission
η_k is the isentropic efficiency
In the figure A.3 are plotted the COPs for the typical days and since just the surface heating has a varying temperature, therefore it is the only one not constant over the time steps.
It's avoided to plot the coefficient when the technology is not turned on.

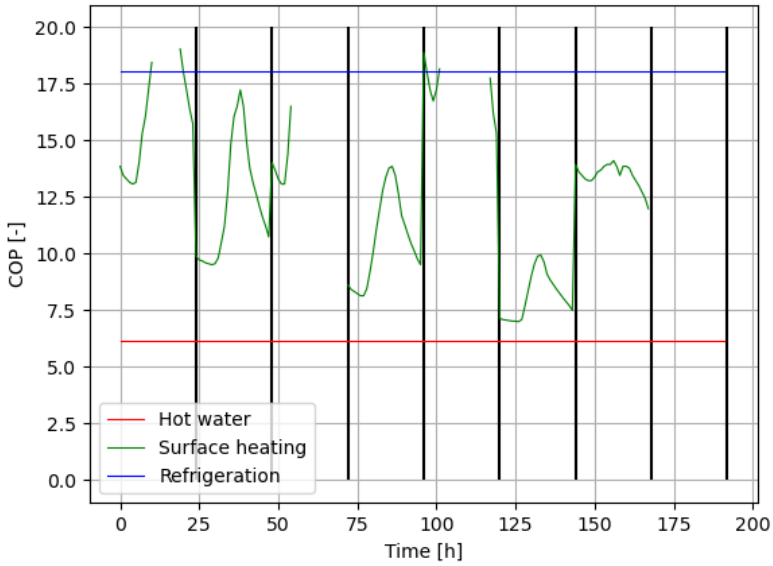

Figure A.3: COP for typical days

A.7.1 Domestic hot water

The domestic hot water heat pump is modelled as a supercritical HP, in order to provide to the buildings water with a temperature of 70°C. Characteristic of the unit:

- Heat pump for the district hot water: it converts a certain quantity of CO_2 from vapour to liquid, since heat needs to be provided to the building.
  Units:

Unit -	F_{min} [t/h]	F_{max} [t/h]	Cost1 [Euro]	Cost2 [Euro/(t/h)]	Cinv1 [Euro]	Cinv2 [Euro/(t/h)]
HP_dhw	0	$F_{max,dhw}$	0	0	Cinv1	Cinv2

Streams:

Type	Layer	In/Out of the layer	Value
$CO2_{dhw,in}$	$CO2_{vap}$	In	massflow
$CO2_{dhw,out}$	$CO2_{liq}$	Out	massflow
$Elec_{dhw}$	elec	In	HP_E

Type	T_{in}	h_{in}	T_{out}	h_{out}	dT_{min}
Heat	T_{cond_in}	HP_{Qc}	T_{cond_out}	0	$dT_{min,ref/ref}$

Parameters:

- Investment cost:

$$C_{inv,1} = Cost_{inv,1} \cdot \frac{i \cdot (1+i)^n}{(1+i)^n - 1} \tag{A.28}$$

$$C_{inv,2} = Cost_{inv,2} \cdot \frac{i \cdot (1+i)^n}{(1+i)^n - 1} \cdot HP_E \tag{A.29}$$

- Energy:

$$HP_E = m \cdot \frac{h_{cond,inlet} - h_{evap,out}}{\eta_{mec}} \tag{A.30}$$

$$HP_{Qc,w} = m \cdot (h_{cond,inlet} - h_{cond,out}) \tag{A.31}$$

- Flow rate:

$$m = 1\, kg/s \tag{A.32}$$

A.7.2 Space heating

A heat pump for providing surface heating is integrated, adopting as working fluid R1234yf. The temperature of the air generated is fuction of the requirements of the buildings and due to the outside temperature.
Characteristic of the unit:

- Heat pump for the district hot water: it converts a certain quantity of CO_2 in the state of liquid, since heat needs to be provided:
  Units:

Unit	F_{min}	F_{max}	Cost1	Cost2	Cinv1	Cinv2
-	[t/h]	[t/h]	[Euro]	[Euro/(t/h)]	[Euro]	[Euro/(t/h)]
HP_sh	0	$F_{max,sh}$	0	0	Cinv1	Cinv2

Streams:

Type	Layer	In/Out of the layer	Value
$CO2_{dhw,in}$	$CO2_{vap}$	In	massflow
$CO2_{dhw,out}$	$CO2_{liq}$	Out	massflow
$Elec_{dhw}$	elec	In	HP_E

Type	T_{in}	h_{in}	T_{out}	h_{out}	dT_{min}
Heat	T_{cond_in}	HP_{Qc}	T_{cond_out}	o	$dT_{min,ref/ref}$

Parameters:

- Investment cost:

$$C_{inv,1} = Cost_{inv,1} \cdot \frac{i \cdot (1+i)^n}{(1+i)^n - 1} \tag{A.33}$$

$$C_{inv,2} = Cost_{inv,2} \cdot \frac{i \cdot (1+i)^n}{(1+i)^n - 1} \cdot HP_E \tag{A.34}$$

- Energy:

$$HP_E = m \cdot \frac{h_{cond,inlet} - h_{evap,out,superheated}}{\eta_{mec}} \tag{A.35}$$

$$HP_{Qc,w} = m \cdot (h_{cond,inlet} - h_{cond,out,subcooled}) \tag{A.36}$$

- Flow rate:

$$m = \frac{h_{evap} - h_{cond}}{h_{evap,outlet,superheated} - h_{expansionvalve,outlet}} \tag{A.37}$$

A.7.3 Refrigeration

A heat pump for providing refrigeration to the buildings, using as working fluid R1234yf. The air temperature that is provided to the buildings is constant at 16°C.
Characteristic of the unit:

- Heat pump for the refrigeration: it converts a certain quantity of CO_2 in the from liquid to vapour, since heat needs to be provided:
  Units:

Unit -	F_{min} [t/h]	F_{max} [t/h]	Cost1 [Euro]	Cost2 [Euro/(t/h)]	Cinv1 [Euro]	Cinv2 [Euro/(t/h)]
HP_{Qc}	0	$F_{max,ref}$	0	0	Cinv1	Cinv2

Streams:

Type	Layer	In/Out of the layer	Value
$CO2_{ref,in}$	$CO2_{liq}$	In	massflow
$CO2_{ref,out}$	$CO2_{vap}$	Out	massflow
$Elec_{ref}$	elec	In	HP_E

Type	T_{in}	h_{in}	T_{out}	h_{out}	dT_{min}
Heat	T_{evap_in}	0	T_{evap_out}	HP_{Qe}	$dT_{min,ref/CO_2}$

Parameters:

- Investment cost:

$$C_{inv,1} = Cost_{inv,1} \cdot \frac{i \cdot (1+i)^n}{(1+i)^n - 1} \tag{A.38}$$

$$C_{inv,2} = Cost_{inv,2} \cdot \frac{i \cdot (1+i)^n}{(1+i)^n - 1} \cdot HP_E \tag{A.39}$$

- Energy:

$$HP_E = m \cdot \frac{h_{cond,inlet} - h_{evap,out,superheated}}{\eta_{mec}} \tag{A.40}$$

$$HP_{Qe} = m \cdot (h_{evap,out,superheated} - h_{expansionvalve,outlet}) \tag{A.41}$$

- Flow rate:

$$m = \frac{h_{evap} - h_{cond}}{h_{condenser,inlet} - h_{condensation,outlet,subcooled}} \tag{A.42}$$